Colorimetric Identification of Proteins Using Gold Nanoparticles

by

Jacob Laurence Rogowski

A thesis

presented to the University of Waterloo

in fulfilment of the

thesis requirement for the degree of

Master of Applied Science

in

Chemical Engineering (Nanotechnology)

Waterloo, Ontario, Canada, 2016

AUTHOR'S DECLARATION

I hereby declare that I am the sole author of this thesis. This is a true copy of the thesis, including any required final revisions, as accepted by my examiners.

I understand that my thesis may be made electronically available to the public.

Abstract

Proteins are the principal executive biomolecules of life. Their existence is required to drive and regulate countless physiological and biochemical activities within the cell. The study of biochemistry and biology are therefore frequently concerned with monitoring the presence, distribution, and function of proteins. Conventional protein identification assays are often labour-intensive and rely on the use of expensive antibodies. The development of new protein biosensors that incorporate nanotechnology, specifically gold nanoparticles (AuNPs), may allow for facile detection, identification, and quantification of proteins due to their colorimetric output. Unlike other strategies that use antibody-functionalized gold nanoparticles, the pairing of non-functionalized nanoparticles with spectroscopic analysis may further reduce the cost of analysis and make this technology viable for consumer-level applications.

This thesis focuses on the development of a gold nanoparticle biosensor for the detection, identification, and quantification of proteins. The underlying principle is based on the aggregation of non-functionalized gold nanoparticles in the presence of proteins. The physicochemical characteristics of these gold nanoparticles can be manipulated to alter their response to different proteins. In order to achieve identification based on non-specific interactions, a "chemical nose" strategy is followed, whereby different gold-nanoparticles produce different individual responses, and their collective response defines a unique signature for a given protein. A review of current literature presents the variety of biological, chemical, and physical factors that can affect protein-nanoparticle interactions, and their resultant effect on colloidal stability. This review also highlights the complexity with which these factors can interact and identifies key considerations for maintaining or controlling colloidal stability in various applications.

The experiments herein address the role of shape and surfactant-type on aggregation of gold nanoparticles. Shape has previously been shown to affect protein-nanoparticle interactions, but to our knowledge has not been exploited for protein sensing applications. The role of surfactant on protein-gold nanoparticle interactions is not well studied and provides a novel avenue for investigation. This work demonstrates that both these parameters can be used to alter protein-nanoparticle interactions, thereby permitting "chemical nose"-type detection of proteins. Overall, these studies highlight how modifying protein-nanoparticle interactions can be used for the benefit of biosensing in research and clinical settings. In addition to biosensing, this manner of investigation can serve as a powerful tool to study protein-nanoparticle interactions, with widespread implications in medicine, environmental protection, and water treatment.

Acknowledgements

First and foremost, I thank my supervisor, Professor Frank Gu, for his support, guidance, and advice throughout my research. The training I received in his laboratory has been invaluable in my personal and scientific development.

Within our research group, I would like to extend my appreciation to all the students, past and present, who make our research group warm and welcoming. In particular, I am indebted to Dr. Mohit Verma for his constant mentorship and support in all aspects of my research. I would also like to extend special thanks to Paul Chen, Sarah LeBlanc, Erin Bedford, Shengyan (Sandy) Liu, Stuart Linley, and Timothy Leshuk.

I would also like to thank those research groups and individuals who have provided help or resources throughout this project. Namely, I would like to thank Yong (Frank) Ding from Professor Pu Chen's lab for his help with zeta potential measurements.

Finally, I would like to recognize the financial support I received during my research. I thank the National Sciences and Engineering Research Council of Canada (NSERC) Canada Graduate Scholarship – Master's program, the Waterloo Institute of Nanotechnology (WIN) Nanofellowship, and the University of Waterloo's President's Graduate Scholarship.

Dedication

To my family and fiancée

For your endless love, support, and encouragement

Table of Contents

List of Figures

List of Tables

List of Equations

List of Abbreviations

AGR   *Albumin/globulin ratio*

AMG   *Amyloglucosidase*

AuNP   *Gold nanoparticle*

BCA   *Bicinchoninic acid assay*

BSA   *Bovine serum albumin*

CTAB   *Cetyltrimethylammonium bromide*

DLS   *Dynamic light scattering*

DLVO   *Derjaguin-Landau-Verwey-Overbeek*

ELISA   *Enzyme-linked immunosorbent assay*

Fib   *Fibrinogen*

GB1   *Protein G B1 domain*

GB3   *Protein G B3 domain*

GFP   *Green fluorescence protein*

Hgb   *Hemoglobin*

HSA   *Human serum albumin*

IgG   *Immunoglobulin G*

IR   *Infrared*

LSPR   *Localized surface plasmon resonance*

Lyz   *Lysozyme*

MFA   *Multiple factor analysis*

Mw   *Molecular weight*

NP   *Nanoparticle*

OD   *Optical density*

PAA   *Poly(acrylic acid)*

PAGE   *Polyacrylamide gel electrophoresis*

PAH   *Poly(allylamine hydrochloride)*

PBS   *Phosphate buffered saline*

PCA   *Principal component analysis*

PEG   *Poly(ethylene glycol)*

pI   *Isoelectric point*

PMMA   *Poly(methyl methacrylate)*

PRLS   *Plasmon resonant light scattering*

PS   *Polystyrene*

PTT   *Photothermal therapy*

SDS   *Sodium dodecyl sulfate*

SERS   *Surface-enhanced Raman spectroscopy*

TEM   *Transmission electron microscopy*

tTG-IgA   *Tissue transglutaminase G-Immunoglobulin A*

UV-Vis   *Ultraviolet-visible*

VDW   *van der Waals*

Chapter 1
Introduction

1.1 Overview

Proteins play an integral role in countless biochemical processes. Among their roles, they can act as biological catalysts, signalling molecules, or structural components. As such, many clinical tests aim to identify, quantify, or measure the activity of proteins. For instance, high serological levels of tissue transglutaminase antibody (tTG-IgA) are indicative of celiac disease[1], and elevated levels of immunoglobulin G antibodies (IgG) can be used to diagnose autoimmune hepatitis[2]. The ability to reliably detect and quantify proteins is a key part of life science research.

Many conventional protein assays, such as enzyme-linked immunosorbent assay (ELISA), require skilled operators and sensitive antibody reagents. Recent developments in gold nanoparticle-based assays promise not only to simplify this process, but also to improve assay sensitivity and adaptability.[3] Nanoparticles are advantageous for many sensing platforms due to their unique properties including a high surface area-to-volume ratio. Gold nanoparticles in particular also possess unique optical properties. Due to localized surface plasmon resonance (LSPR), the aggregation of gold nanoparticles in solution results in a visible colour change[4]. This allows users to easily track changes in nanoparticle aggregation, which is beneficial for many sensing platforms. By designing gold nanoparticles that change their colour in response to a particular protein or analyte, users can easily read these colorimetric sensors without specialized equipment.

One common strategy for detecting biomolecules with gold nanoparticles is to use nanoparticles with surface-functionalized probes.[5–8] These probes, often antibodies or aptamers, can then interact with proteins in solution to aggregate or stabilize the gold nanoparticles. Given that functionalization of gold surfaces is well studied, this method provides convenient detection of proteins with good specificity. However, production of probe-functionalized gold nanoparticles may be limited by the requirement for specific antibodies, which increase assay cost. Furthermore, antibodies may be sensitive to temperature and pH fluctuations that could hinder their performance and present challenges for consumer-level deployment.

The observation that proteins can induce aggregation of non-functionalized gold nanoparticles has led several groups to investigate the use of probeless nanoparticles for colorimetric protein sensing.[9–11] Unlike probe-functionalized nanoparticles, these nanoparticles change their colloidal stability in

response to many different proteins. Variations in amino acid composition[12], protein identity[13,14], and protein structure[11] generate a unique response from protein to protein. In order to maximize differences in protein-nanoparticle interaction, it can be beneficial to use a variety of different nanoparticles, where each nanoparticle responds differently to a given protein. This type of biosensors, which relies on an array of responses instead of a single output, has been called a "chemical nose".[15] The array of responses allows for greater discrimination between samples when compared to a single output, and harnessing these differences could lead to the development of low-cost broad-spectrum protein sensors.

1.2 Research objectives

The aim of the following project is to investigate the application of non-functionalized gold nanoparticles for "chemical nose" colorimetric detection of proteins. In order to enhance discrimination between proteins, variations in nanoparticle structure, surface properties, and their effect on colloidal stability with proteins is explored. The potential for certain properties to alter protein-nanoparticle interactions was first established from literature review. Based on these findings, the following objectives were established:

1. Demonstrate that cetyltrimethylammonium bromide (CTAB)-coated morphologically-controlled gold nanoparticles produce a colorimetric response in the presence of protein.
   a. Investigate whether the observed response is dependent on protein concentration to evaluate the potential for protein quantification
   b. Investigate whether spherical and branched gold nanoparticles generate different responses to an array of proteins to evaluate the potential for "chemical nose" type array sensing

2. Establish the potential for "chemical nose" protein sensing in complex mixtures
   a. Investigate the possibility of identifying protein mixtures based on the response of single proteins
   b. Determine the ability to detect variations in protein concentration in the complex environment of human serum

3. Develop gold nanoparticles with different surface properties by controlling the presence of surfactants.
   a. Determine whether replacing cationic surfactants with non-ionic or anionic surfactants can change particle surface charge

  b. Determine whether changing the stabilizing surfactant affects the colloidal stability of gold nanoparticles

 4. Expand the capabilities of the "chemical nose" protein biosensor by including surfactant-modified gold nanoparticles
  a. Observe whether changing the stabilizing surfactant alters a nanoparticle's colloidal response to protein
  b. Determine whether protein discrimination is improved with a three-surfactant array
  c. Investigate the effect of surfactant concentration on protein-induced nanoparticle aggregation

1.3 Thesis outline

This thesis is comprised of five sections including one general introduction to the research topic, one section of literature review, two sections of experimental research, and a conclusion which summarizes the work and provides future outlooks.

Chapter 1 provides an overview of the research topic and questions which will be addressed through literature review and/or experimental approaches. This section also helps outline the framework of the thesis.

Chapter 2 consists of a literature review on the subject of gold nanoparticle-protein interactions, their effects on colloidal stability of gold nanoparticles, and the significance of these interactions on various nanotechnology applications. Given the vast potential for gold nanoparticles to improve biosensing, diagnostic, and treatment applications in clinical and research settings, their interactions with proteins have come under considerable investigation in recent years. However, as is shown in this review, the complex interactions between biological, chemical, and physical factors can lead to debate as to their effects on colloidal stability. Here, we compile current research, identify key aspects of protein-nanoparticle interactions, and discuss their potential interactions. In doing so, we seek not only to help in interpreting conflicting results, but also to identify new avenues of investigation.

Chapter 3 presents the first development of a gold nanoparticle "chemical nose" sensor capable of identifying and quantifying proteins in solution. Here, we leverage the impact of gold nanoparticle morphology on protein-nanoparticle interactions. By mixing various protein solutions with spherical and branched gold nanoparticles, we observe differences in colloidal stability that are sensitive to both protein concentration and identity. This technique is also used to distinguish between various protein

mixtures and complex media, supporting possible applications for clinical and diagnostic applications. These experiments lay the foundation for this protein sensing "chemical nose" technique.

Chapter 4 expands on previous "chemical nose" techniques by investigating the role of surfactant on colloidal stability of gold nanoparticle-protein solutions. We first observe that altering the surfactant in which gold nanoparticles are stabilized can be achieved using a facile surfactant replacement procedure. Critically, we established that changes in surfactant can radically alter the aggregation response of gold nanoparticles to proteins. To our knowledge, this is the first time this relationship between stabilizing surfactant and protein-gold nanoparticle interactions has been investigated and the findings stand to significantly affect the development of future nanoparticle systems.

Finally, chapter 5 provides a summary of conducted research and experiments which comprise this thesis and key conclusions which can be drawn from our findings. We also identify future directions for improving this technology and expanding the application of gold nanoparticles for protein sensing and identification.

Chapter 2
Literature Review

2.1 Summary

Gold nanoparticles are among the most popular materials in nanobiotechnology. Their unique optical properties, facile surface functionalization, and biocompatibility make them a versatile platform for sensing, diagnostic, and therapeutic applications. In many cases, controlling the colloidal stability of gold nanoparticles is vital for optimal performance. Particles which aggregate too readily or do not aggregate when needed are both examples of undesirable behavior. While specific interactions between proteins and functionalized antibodies or aptamers are commonly used to stabilize or aggregate gold nanoparticles, it has been known for some time that proteins can adsorb non-specifically to gold nanoparticles, thereby inducing changes in their colloidal stability. Unfortunately, this aspect is often overlooked when discussing their application. Given the ubiquitous nature of proteins in biological samples, this represents a significant gap in the development of reliable gold nanoparticle systems. While recent investigations have started to identify factors affecting protein-gold nanoparticle interactions, the multitude of factors and variations between studies makes interpretation of findings difficult. Here, we review the effect of non-specific protein-nanoparticle interactions on colloidal stability of gold nanoparticles. First, we provide an overview of physicochemical factors which can affect protein-gold interactions. Then we discuss recent studies into their effect on nanoparticle aggregation and stability. Finally, we put these factors in context with several examples of sensing, diagnostic, and therapeutic applications which are heavily influenced by these effects. Understanding how proteins can affect the colloidal stability of gold nanoparticles is an important aspect for developing reliable applications.

2.2 Introduction

Gold nanoparticles have experienced a dramatic increase in popularity over the past several years as researchers aim to harness their unique physical and chemical properties for a wide range of sensing, diagnostic, and therapeutic applications. These metallic nanoparticles exhibit several attractive characteristics which make them especially promising for life science research. Among these characteristics are large surface areas with well known methods for molecule attachment[16], relatively low cytotoxicity and good biocompatibility[17], well characterized synthesis procedures capable of controlling nanoparticle morphology[18], and unique optical properties which facilitate analysis[4,19].

The ability to control nanoparticle aggregation is central to many applications.[20] In certain scenarios, such as cellular uptake and catalysis, aggregation of gold nanoparticles is undesirable since it can alter their behavior and reduce available surface area. In other scenarios, controlled aggregation in response to biological, chemical, or physical cues is desirable as a method of colorimetric detection.[20] Regardless of the particular application, careful consideration must be given to the colloidal stability of gold nanoparticles to ensure they maintain their desired function.

While specific interactions between probe-functionalized gold nanoparticles and their respective proteins are comparatively easy to predict and extensively studied, the study of non-specific interactions between proteins and gold nanoparticles is just starting to increase in popularity. These interactions are often unplanned and exist as a consequence of having proteins in solution. It is well known that non-specific interactions between a variety of materials and proteins modulate both the physical characteristics and behavior of nanoparticles.[21] The ubiquitous nature of proteins in biological media means that gold nanoparticles in biological samples will almost certainly be influenced by one or more proteins. While recent years have produced a substantial body of evidence linking the interaction of proteins and gold nanoparticles to colloidal stability, the absence of systematic investigations means that effects must be interpreted on a case by case basis. Furthermore, it is not uncommon for similar studies to reach conflicting conclusions based on slight variations in experimental detail. A prominent example is the ability of certain proteins to both stabilize[9,22], and aggregate[11,23] similar gold nanoparticles. These findings are likely dependent on many experimental factors which were not the primary focus of the study (e.g. ionic strength, particle morphology, protein conformation). Understanding the potential interference of these factors is a necessary step in drawing useful conclusions.

The non-specific adsorption of proteins on the gold nanoparticle surface is often part of the putative mechanism for particle aggregation or stabilization. As such, much of this review is also concerned with protein adsorption on nanoparticle surfaces. The adsorbed protein layer is commonly referred to as the "protein corona" and contributes largely to defining the nanoparticle's "biological identity" as well as its physical characteristics. Three major phenomena that play key roles in protein corona formation are thiol-gold bonding[12,24], hydrophobic bonding[22], and electrostatic interactions[25]. Given the intimate connections between different experimental conditions that affect these phenomena, it is impossible to discuss them in isolation. However, for the purpose of this review, they can be roughly grouped into two themes: charge and structure. Charge factors such as particle zeta potential and protein isoelectric point have long been used to explain protein-nanoparticle interactions, while the importance of structure-based factors such as particle morphology and protein conformation have only recently gained

attention. The environment in which proteins interact with nanoparticles has been shown to play a crucial role in determining nanoparticle stability[26–28], therefore factors such as ionic strength[29], surfactants[30], pH[31,32], and temperature[33] cannot be overlooked.

This complexity of protein-nanoparticle interactions has led some to claim that general laws for protein adsorption are unlikely to exist.[34] Yet, the ability to predict and control colloidal stability of gold nanoparticles in the presence of proteins is invaluable in the pursuit of novel applications. Herein we will outline several key factors identified in recent studies on protein-gold nanoparticle interactions as well as their potential effects on gold nanoparticle stability. We will also discuss some practical considerations concerning the performance of sensing, diagnostic, and therapeutic assays based on gold nanoparticles.

2.3 Factors affecting protein-gold nanoparticle interactions

2.3.1 Charge

Electrostatic forces are often cited as the most influential factor in protein adsorption and nanoparticle stability. A zeta potential of $\pm$ 30 mV is typically considered sufficient to prevent nanoparticles in aqueous solution from aggregating due to electrostatic repulsion. The magnitude of the electrostatic force (F_e) between two electrically charged particles is described in its simplest form by Coulomb's law,

$$F_e = k_e \frac{q_1 q_2}{r^2} \qquad \text{(Eq. 2.1)}$$

where q_1 and q_2 are the point charges of two particles, r is the separation distance, and k_e is Coulomb's constant (~ 8.99 x 10^9 Nm^2C^{-2}). The magnitude of this interaction force is therefore proportional to the charges q_1 and q_2, and is inversely proportional to the square of the separation distance. If the product of q_1 and q_2 is positive, $F_e > 0$ and the force is repulsive. If the product is negative, $F_e < 0$, and the force is attractive. Based on this model, electrostatic forces between like charged nanoparticles will contribute a repulsive force, stabilizing the colloid. In reality, the presence of ions in aqueous media leads to the formation of an electrostatic double layer, resulting in a screened-Coulomb interaction which can reduce stability.[35–37] Furthermore, van der Waals (VDW) forces also modulate interaction of particles in solution.[37,38] The summative effect of these forces on colloidal stability is often approximated using the familiar Derjaguin-Landau-Verwey-Overbeek (DLVO) theory.

Similarly, the strength and direction of electrostatic force between proteins and nanoparticles depends on the net charge and charge distribution of both bodies. Unless the gold nanoparticle surface

7

is completely bare, its surface charge will be largely dependent on the nature of adsorbed monolayers or stabilizing agents. Common methods for stabilizing gold nanoparticles include citrate ions, ionic and non-ionic surfactants, and polymeric coatings (e.g. poly(ethylene glycol)(PEG), poly(acrylic acid)(PAA), poly(allylamine hydrochloride)(PAH)). Depending on which method is used, nanoparticles can have negative, neutral, or positive surface charges which govern their electrostatic behavior. Several studies report electrostatic attraction to be the primary mechanism for adsorption of charged proteins on oppositely charged gold nanoparticles.[10,39] Unlike thiol-gold and van der Waals interactions which are relatively short-ranged effects that contribute strongly to adhesion near the gold surface, the long-range nature of electrostatic forces could facilitate transport of proteins towards the surface.[37] Nevertheless, adsorption is sometimes reported for like-charged proteins and nanoparticles[40], indicating that opposite charge is not a requirement.

2.3.1.1 pH

The charge of amino acids, like other amphiprotic molecules, is sensitive to environmental conditions due to the loss or gain of protons. The protonation state of any single amino acid residue is a function of pH and the acid dissociation constant (pKa) for its functional group. The net charge of a protein is determined by the ratio of positively and negatively charged functional groups. The isoelectric point (pI) of a protein is the pH at which charges are balanced and the protein adopts a neutral charge. Increasing the pH above the pI will lower the concentration of protons and promote deprotonation of amino acid residues, resulting in negatively charged proteins. Conversely, lowering the pH below the pI will promote protonation and yield positively charged proteins. As such, the net charge of a protein depends largely on its amino acid sequence and the solution pH.

Given that electrostatic charge is one of the primary factors that drive protein-gold nanoparticle interactions, it is not surprising that changing the solution pH can affect protein adsorption. A study proposing the application of citrate-capped gold nanoparticles for detection of urinary lysozyme (Lyz) has shown that the amount of gold nanoparticle aggregation is sensitive to solution pH.[10] At pH 7, lysozyme carries a net positive charge (pI = 11) and induces aggregation of negatively charged gold nanoparticles. Incremental increases in pH between 3 and 11 resulted in decreased nanoparticle aggregation as monitored by plasmon resonant light scattering (PRLS).[10] This aggregation was not simply due to a decrease in nanoparticle stability at low pH since no variations in PRLS were observed in the absence of lysozyme. Furthermore, at a pH of 10 and 11, the PRLS of gold nanoparticles with lysozyme was comparable to those without the protein, which suggests that neutrally charged lysozyme does not induce aggregation of anionic citrate-capped gold nanoparticles. This pH-dependent

electrostatic adsorption model is consistent with studies by Pan et al. which noted that adsorption rate constants between Protein G B1 domain (GB1) and negatively charged latex particles were highest when solution pH conferred a strong net positive charge to GB1.[41]

Since gold nanoparticle-protein solutions appear to aggregate more readily when proteins and nanoparticles are oppositely charged, it is possible that changes in protein identity, amino acid sequence, and post-translational modifications can affect whether aggregation is observed. Using chemical modification of amino acids in three proteins with different pIs, one group has confirmed that changes in protein charge affect whether they caused aggregation of gold nanoparticles.[39] In this study, lysozyme, α-lactalbumin, and myoglobin were modified either by succinylation, acetylation, or aminoalkylation to change the charge on particular residues. Upon incubation with negatively charged gold nanoparticles, aggregation was only observed when proteins were positively charged (at pH values lower than the new pI of the modified protein). These findings support the idea that gold nanoparticle stability in the presence of proteins is highly dependent on solution pH.

Variations in pH can also affect the surface charge of nanoparticles coated with organic molecules. If gold nanoparticles are functionalized with amphiprotic peptides or PEG, their colloidal stability can be affected by charge neutralization.[27] Here, neutralization of carboxylic acid groups at pH < 5 was shown to cause nanoparticle aggregation when the electrostatic repulsive force was decreased.
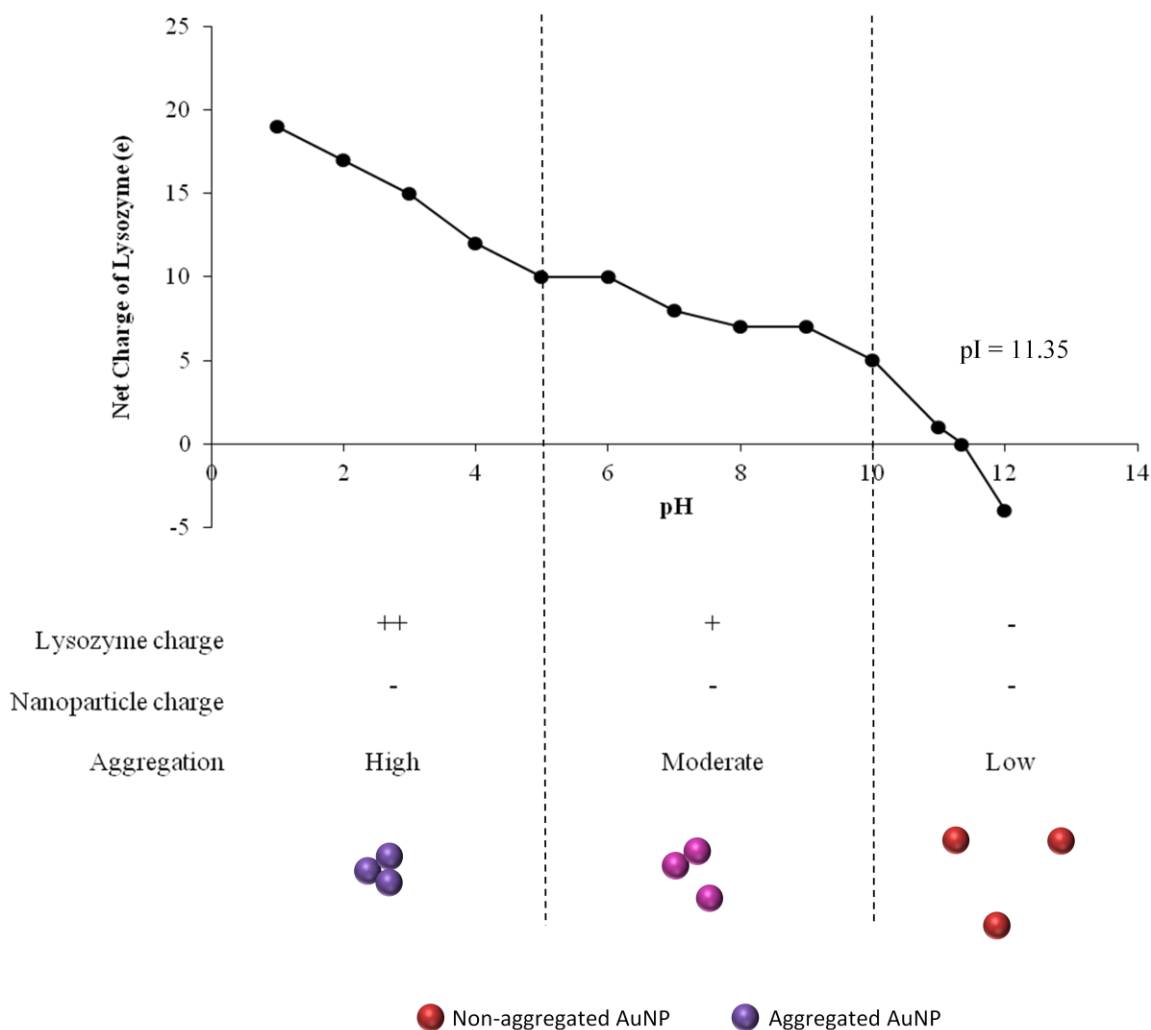
Figure 2.1 pH dependent lysozyme charge and aggregation of citrate-capped gold nanoparticles. Adapted from Yu et al. 2015[42], and Wang et al. 2010[10].

2.3.1.2 Ionic Strength

It is generally well known that gold nanoparticle suspensions can be induced to aggregate under conditions of high ionic strength.[7,35,43,44] As an example, Pamies et al.[35] observed that addition of 75 mM sodium nitrate salts to suspensions of citrate-stabilized gold nanoparticles was sufficient to induce the formation of aggregates. The overall colloidal stability was inversely proportional to ionic strength.[35] This relationship between ionic strength and colloidal stability is by no means exclusive to gold nanoparticles, as similar behavior has been characterized in other materials such as silver[45,46], polystyrene[47], and numerous metal oxides[48-50].

The influence of ionic strength on protein-gold nanoparticle binding experiments is often overlooked or not reported, despite evidence showing that ionic strength can influence the adsorption of proteins onto gold surfaces. One study found that binding constants for bovine serum albumin (BSA) on gold nanorods were different in MOPS buffer and pure water.[51] A study on negatively charged latex particles suggests similar dependence between GB1 adsorption and ionic strength where varying NaCl concentration from 70 mM to 200 mM caused a significant decrease in association rate.[41] These findings are consistent with the common model for charge-screened interactions, whereby electrostatic forces between charged bodies are reduced by electrostatic double layer formation. These changes in protein adsorbance can ultimately affect the stability of gold nanoparticles by altering corona thickness, surface coverage, and corona composition when proteins have different pIs.

Adsorption of biomolecules is sometimes used to prevent aggregation of nanoparticles under high salt concentrations.[45,46,52] For proteins, this is often explained by the formation of a protein corona which provides steric stability when high salt concentrations screen electrostatic repulsion.[53] Since steric stabilization by surface-attached polymers such as PEG produces nanoparticles which are already stable under high ionic strength[54,55], this effect is presumably greatest for those charged nanoparticles which rely predominantly on electrostatic repulsion.

In addition to the inherent destabilizing effect of certain ions and their effect on protein adsorption, salts can alter long-distance interactions between non-adsorbed proteins and nanoparticles. One group that observed BSA contributing to depletion-aggregation of gold nanoparticles decorated with ethylene glycol noted that addition of 0.3M NaCl increased the rate of nanoparticle aggregation and decreased the critical protein concentration necessary to cause aggregation.[38] In this case, the presence of ions was thought to screen the surface charge of proteins and enhance the depletion effect. Further studies by the same group confirmed that electrostatic repulsion presents a significant energy barrier to nanoparticle aggregation at low salt concentrations, and that charge screening at high salt concentrations makes particles aggregate faster in a diffusion-limited process.[56]

2.3.2 Structure

2.3.2.1 Nanoparticle morphology

Gold nanoparticles can be synthesized in a variety of different sizes and shapes. Due to localized surface plasmon resonance, shape and size affects the electromagnetic absorbance spectrum of gold colloids. For example, larger particles usually exhibit absorbance peaks at longer wavelengths.[57–59] Aggregation of gold nanoparticles can also cause a red-shift in their absorbance spectrum.[4] This

property is commonly used for colorimetric sensing applications to produce nanoparticle solutions with different colours where colour change reflects particle size or aggregation state. Along with size control, varying shape anisotropy is a common method for modifying the optical and physical characteristics of gold nanoparticle suspensions.[59] Cubic[60–62], pyramidal[60,62,63], rod-shaped[60,62–64], and branched gold nanoparticles[60,62,65,66], have all been reported in literature, and shape has a direct effect on the absorbance spectrum[59]. For example, gold nanorods with higher or lower aspect ratios can be synthesized using seed-mediated growth in the presence of a template surfactant.[60] The resultant particles exhibit two LSPR peaks reflecting the longitudinal and transverse dimensions of the rod.[30,67] In addition to varying optical characteristics, the variety of particle sizes and shapes may also affect how particles interact with adsorbed proteins and their resultant colloidal stability. As such, it is important to acknowledge that nanoparticle morphology can affect their behavior in biological media.

Cytochrome c was found to prevent salt-induced aggregation of citrate-stabilized gold nanoparticles between 2 nm and 41 nm in diameter.[68] However, stability was only observed when the number of cytochrome c molecules per nanoparticle exceeded a certain size-dependent threshold. Larger nanoparticles required more cytochrome c molecules to become stabilized than smaller nanoparticles. Jiang et al.[68] also concluded that electrostatic forces dominate the adsorption mechanism of cytochrome c onto 16 nm particles, while hydrophobic forces dominate on smaller 2-4 nm particles, based on the observed ratio of α-helix and random coil structure as well as the position of a positively charged grove rich in lysine. In surveying an array of common human blood proteins (i.e. γ-globulin, fibrinogen (Fib), insulin, human serum albumin (HSA), and histone) and their interactions with citrate-stabilized gold nanoparticles, de Paoli et al.[69] also observed the size-dependent formation of protein coronas and protein-nanoparticle aggregates. As particle size increased from 5 nm to 60 nm, a general increasing trend in association constant between each protein and the nanoparticle surface was observed. Above 60 nm, the trend continued for globulins and insulin, while albumin, fibrinogen, and histone association constants remained approximately the same or decreased slightly. This increase in association constants was associated with an increase in protein corona thickness. A similar study investigating the role of PEG grafting density and nanoparticle size (15-90 nm) on adsorption density of serum proteins found that protein density was higher on smaller particles, presumably owing to reduced steric interaction on highly curved surfaces.[70] This relationship between density of protein coverage and particle size is especially important for colloidal stability of nanoparticles in cases where aggregation is believed to be caused by bridging flocculation, such as in the case of fibrinogen binding to poly(acrylic acid) coated gold nanoparticles[71]. Here, it was proposed that fibrinogen can induce aggregation of gold nanoparticles large enough to bind multiple protein molecules. Size of gold nanoparticles can also affect their

colloidal stability when particles are protected from protein adsorption. As previously mentioned, when gold nanoparticles of various sizes were decorated with ethylene glycol and incubated with BSA, depletion aggregation was found to drive aggregate formation.[38] In addition to the charge-screening effect, the authors also noted that the critical protein concentration required to induce aggregation was much higher for small nanoparticles, and proposed that large particles experience higher osmotic pressures which drive them together.

While some studies have sought to characterize how nanoparticle shape influences protein adsorption, the role of particle shape in protein-induced aggregation remains poorly understood. A common theme among studies is the role of nanoparticle shape in changing protein conformation. This relationship was demonstrated by incubating positively charged lysozyme and α-chymotrypsin with negatively charged (16-mercaptohexadecanoic acid-stabilized) spherical and rod-shaped gold nanoparticles.[14] While the number of adsorbed proteins per spherical particle was similar for lysozyme and α-chymotrypsin, both proteins adhered in greater numbers to rod-shaped proteins. Particle surface area was noted as a potential reason for this difference; however the three-fold increase in surface area is appreciably lower than the change in protein density which increased more than eight-fold. Also, while both proteins were similar in molecular weight and dimensions, their adsorption and conformational changes differed.[14] The authors attributed these differences to variations in secondary structure and isoelectric point, highlighting the importance of protein identity on nanoparticle aggregation. It was proposed that nanoparticle aggregation occurs due to the binding interaction of structurally altered proteins on adjacent nanoparticles. Aggregation is therefore determined by the propensity of a particular protein identity to change its conformation upon adsorption to a gold surface, and this propensity is influenced by nanoparticle shape. Thick protein coronas may result in stable particles if underlying proteins shield the outermost layer from the denaturing effects of the gold surface.[14]

A similar investigation into BSA interactions with spherical and rod-shaped cetyltrimethylammonium bromide (CTAB)-coated gold nanoparticles revealed that BSA underwent a conformational change and loss of function upon binding to rod-shaped particles. This denaturation was not observed with spherical particles [33]. However, the LSPR absorbance peaks for both particle shapes exhibited broadening characteristic of gold nanoparticle aggregation. When comparing the effect of three similarly sized nanoparticles of different shapes (spheres, rods, and triangles) on BSA adsorption, Chaudhary et al.[40] observed that BSA bound most strongly to spherical gold nanoparticles, followed by rod shaped, and finally triangular particles. Interestingly, the authors did not identify any nanoparticle aggregation, regardless of particle shape or protein denaturation. Together, these findings suggest not

13

only that gold nanoparticle shape is an important factor in protein adsorption, protein denaturation, and colloidal stability, but also that loss of protein conformation is neither sufficient nor required for aggregate formation.

2.3.2.2 Protein conformation and composition

It is clear that interactions between gold nanoparticles and proteins are highly dependent on the identity of the protein. Several studies observed differences in protein adsorption and resultant nanoparticle aggregation when assaying different proteins.[11,13,14] These differences are not surprising given the diversity of proteins with respect to size, shape, chemical composition, charge and hydrophobicity. The primary structure of a protein is defined by its sequence of amino acids and their corresponding functional groups. Whether these groups are exposed and accessible for direct interaction (e.g. with the gold surface) is determined by secondary, tertiary, and quaternary structure. Since changes in protein conformation can rearrange these features and change the physicochemical nature of the protein surface, conformation likely plays a key role in protein-nanoparticle interactions that can lead to stability or aggregation of gold colloids.

The strong bonding interaction between the sulfur atom of thiol groups (-SH) and gold surfaces is a popular tool in the preparation of self-assembled monolayers. Cysteine is the only naturally occurring amino acid which contains a thiol group. As such, several studies into protein-gold interactions have investigated the role of cysteine residues in protein adsorption and nanoparticle aggregation.[11,12,24,72] Generally, cysteine residues are believed to contribute most strongly when they are accessible at the protein surface and not buried within the core of globular proteins or occupied in disulfide bonds. A recent study by Thioune et al.[72] investigated the degree of interaction between gold nanorods and four different globular proteins by monitoring changes in the LSPR characteristic of nanoparticle aggregation. They found that the number of solvent-accessible thiol groups per protein is a contributing factor in the observed LSPR shift. It was also proposed that their spatial distribution on the exposed surface is critical since neighbouring cysteine residues can behave as one due to steric accessibility and exposed cysteines on opposite sides of the protein could potentially bridge two nanoparticles, thus forming strong aggregates. While some studies have found that presence of cysteines does not contribute strongly to initial adsorption of proteins, it is generally accepted that they solidify the attachment and contribute to irreversible "hard" corona formation[12,24]. Siriwardana et al.[12] demonstrated this effect by bioengineering Protein G B3 domain (GB3) to contain 0, 1, or 2 cysteine residues. While

the absence of cysteine had no effect on binding kinetics, GB3 without cysteine was readily displaced from the nanoparticle surface, unlike variants with 1 or 2 cysteines.

Amine groups are also capable of strong bonding to gold. Primary amines in particular have been shown to bind strongly to gold crystals.[73] When incorporated into a polypeptide chain, four amino acids (arginine, lysine, asparagines, and glutamine) retain primary amines in their side chains, allowing them to potentially interact with gold surfaces as part of a complete protein. Isothermal calorimetry has been used to quantify the binding strength of lysine and aspartic acid to gold nanoparticles.[74] The side chain of aspartic acid does not have an amine group; however the free amino acid has an N-terminal primary amine. While both amino acids were found to bind the gold surface at physiological pH, the strength of the aspartic acid-gold interaction was much higher than the lysine-gold interaction.[74] This difference was attributed to differences in amine group protonation. The authors concluded that when the amine group is protonated, as in the case of lysine (pI ~ 9.4), the interaction is primarily electrostatic, and when the amine group is deprotonated, as in the case of aspartic acid (pI ~ 2.77), the interaction is covalent in nature with undercoordinated atoms on the gold surface.[74] Furthermore, amine groups on lysine can interact with gold surfaces and carboxyl groups in a pH-dependent manner to induce nanoparticle aggregation.[75] These findings suggest that the interaction between proteins and gold nanoparticles is sensitive to the number of amine residues accessible at the protein surface. Furthermore, this interaction was found to be stronger when those groups are deprotonated, echoing the importance of pH as discussed in section 2.3.1.1[75]

Protein conformation can be as important for gold nanoparticle stability as its amino acid composition since denaturation of proteins prior to incubation with gold nanoparticles has been shown to change the amount of resultant gold nanoparticle aggregation. In one study, α-amylase solutions at varying concentrations were incubated with 7.4 nm citrate-stabilized gold nanoparticles with or without prior thermal denaturation.[11] It was shown that denaturation of amylase prior to incubation reduced the amount of nanoparticle aggregation observed. Green fluorescent protein (GFP), amyloglucosidase (AMG), and BSA solutions were also shown to cause LSPR peak-broadening to varying degrees depending on whether the proteins were denatured prior to incubation.[11] It is especially notable that the direction of the effect observed for α-amylase and GFP was opposite that of BSA and AMG. In other words, denatured BSA and AMG caused more peak broadening and aggregation than their native counterparts. Despite the focus on surface accessible thiol and amine groups in native proteins, it should be noted that protein denaturation could expose groups which were previously inaccessible.[11] Since there are several examples where adsorption of proteins changes their conformation[14,33,68,76], this mechanism may contribute significantly to the aggregation process. These observations highlight how

the role of protein conformation on colloidal stability of gold nanoparticles has to be considered within the context of protein identity.

If protein conformation plays a defining role in nanoparticle stability, then the amount of aggregation observed will likely be sensitive to extreme temperatures, since these can cause proteins to partially or completely lose their native conformations. The sensitivity of a particular system to temperature will therefore also be dependent on the thermal stability of the protein in question, with highly stable proteins being less sensitive to extreme temperatures, and vice versa.

Since surfactants are commonly used to stabilize nanoparticles, their interactions with proteins must not be overlooked. Their denaturing effects in particular may affect protein-protein and protein-nanoparticle interactions. Unfortunately, very little research has been conducted into the role of surfactants on nanoparticle interactions and resultant nanoparticle stability. Predicting the effect of different surfactants on protein-nanoparticle stability is a complex issue given the variety of competing effects including nanoparticle stabilization by adsorbed surfactants, protein denaturation by surfactants, and the interaction between proteins and surfactants at the gold surface. In one study, BSA was shown to completely displace CTAB to produce stable gold nanoparticles, which suggests that some level of binding competition occurs between proteins and surfactants at the gold surface.[30] Natural bile salts have also been shown to partially displace β-lactoglobulin from the protein corona of 200 nm gold particles.[77] If competition between protein and surfactant adsorption is a deciding factor in nanoparticle stability, it is likely that presence of strong bonding thiol and amine residues may bias the equilibrium towards protein corona formation.

2.3.3 Additional factors

2.3.3.1 Protein concentration

Unsurprisingly, the concentration of proteins in solution has repeatedly been found to correlate with colloidal stability of gold nanoparticles. However, the relationship between concentration and stability remains difficult to predict. Interactions between other variables such as particle size, material, shape, surface chemistry, and protein identity make comparison between studies difficult. Different groups have reported positive[9,14,78], and negative[11,33] correlations between protein concentration and colloidal stability. For example, adsorption of cytochrome c onto gold sol particles was found to prevent electrolyte-induced aggregation, but only when the number of protein molecules per nanoparticle exceeded a certain threshold.[68] This threshold was related to particle size as described in section 2.3.2.1. Several other studies have also investigated how the formation of a protein corona can stabilize gold

nanoparticles under conditions otherwise known to cause aggregation.[9,22,26,30] The opposite effect has also been observed, whereby stable gold nanoparticles aggregate with increasing protein concentrations.[10,11,13,72,79] The relationship between protein concentration and colloidal stability is not always linear. In several cases, distinct aggregation regimes have been observed for high, intermediate, and low protein concentrations. For example, an investigation by Deng et al.[71] into the interaction of human fibrinogen with PAA-coated gold nanoparticles suggests that while intermediate concentrations of fibrinogen can aggregate nanoparticles by forming inter-particle bridges, sufficiently high concentrations of fibrinogen formed stabilizing coronas around each particle. Similar patterns in spectral absorbance were observed for citrate-stabilized gold nanoparticles[80]. This model was also proposed by a group studying the interaction of polystyrene (PS) and poly(methyl methacrylate) (PMMA) particles with IgG and fibrinogen.[81] In these three studies, the bell-shaped response was attributed to the steric stabilizing nature of thick protein coronas. An alternative explanation has been proposed by one group, where protein-protein interactions dominate at high protein concentrations and the number of protein-nanoparticle interactions is effectively reduced.[72]
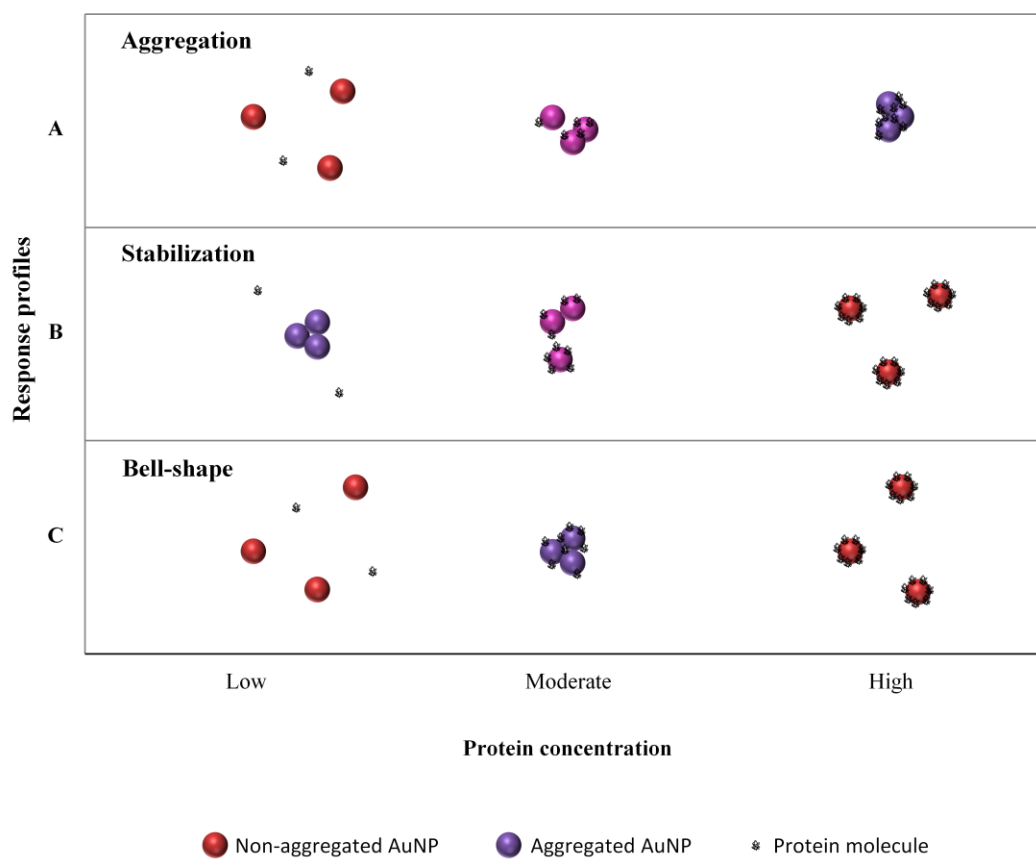
Figure 2.2 Protein concentration-dependent response of gold nanoparticle aggregates. a) Protein-induced aggregation. b) Protein-induced stabilization against salt. c) Bell-shaped response to high and low protein concentrations.

When determining the effect of protein concentration on nanoparticle aggregation, the method by which researchers adjust protein concentration is also vitally important since protein-nanoparticle aggregation is generally irreversible[11,27]. In cases where protein concentration is increased gradually by addition of protein to gold nanoparticles[11], stabilization may never be observed since particles become irreversibly aggregated at moderate protein concentrations. If proteins of the corona are loosely bound to the surface, the inverse behavior might also be observed, whereby stabilized nanoparticles aggregate permanently as protein concentration is decreased, regardless of how much protein is removed. It is therefore important to consider that fluctuations in protein concentration may lead to irreversible aggregation, even if they are returned to stable conditions.

2.3.3.2 Protein mixtures

Studying the effect of protein concentration on gold nanoparticle stability can be further complicated by protein mixtures. With the introduction of other biomacromolecules, the response of gold nanoparticles to proteins can change given new possibilities for protein-protein and protein-nanoparticle interactions. Multiple protein species with different affinities for gold could also lead to competition for binding at the nanoparticle surface.[34,82] A large difference in binding affinity between proteins may mask the effect of lower affinity proteins if they cannot incorporate into the protein corona or if they are displaced from the surface. Similarly, proteins with similar binding affinities may generate mixed protein coronas[70], producing nanoparticles with novel biological identities and colloidal stability. For example, while the addition of BSA or α-amylase to citrate-stabilized gold nanoparticles has been shown to induce particle aggregation, the effect of α-amylase concentration is dependent on BSA concentration when in a binary mixture.[13]

The aggregating or stabilizing properties of proteins in mixtures can be further affected by protein-protein interactions before or during interaction with the nanoparticle surface. For instance, one study which used the aggregation of negatively charged gold nanoparticles to detect positively charged lysozyme noted that strong electrostatic interactions between HSA (a negatively charged protein common in urine samples) and lysozyme could interfere with electrostatic interactions between gold nanoparticles and lysozyme, thereby limiting aggregation.[10]

Given the large number of permutations possible for protein-protein and protein-nanoparticle interactions in complex mixtures, extra care must be given when assessing colloidal stability of gold nanoparticles. Researchers must also be aware that protein effects may not be additive and that interference is commonplace.

2.3.3.3 Polymeric coatings

The nanoparticle surface can be decorated with various coatings. Often, these coatings are aimed at stabilizing particles against salt-induced aggregation, increasing biocompatibility, or reducing biofouling from non-specific protein adsorption. Some organic polymers and polyelectrolytes which have been used with gold nanoparticles include poly(acrylic acid) (PAA)[83], poly(allylamine hydrochloride) (PAH)[51,83] and poly(ethylene glycol) (PEG)[54,84]. PEG is the most popular organic polymer for stabilizing various organic and inorganic nanomaterials since it can provide high levels of colloidal stability as well as improved biocompatibility, an important feature for *in vivo* applications. Many studies have shown that coating gold[85,86] and silver nanoparticles[55] with PEG increases their stability in aqueous media of various ionic strengths. Manson et al.[86] observed a positive relationship between the capping density of PEG on gold nanoparticles and their stability. An increased density of PEG on the surface is also likely to increase particle stability in protein solutions by discouraging protein adsorption[70]. Additionally, coating with polyelectrolytes such as PAA and PAH can confer a strong positive or negative zeta potential which contributes to electrostatic particle behavior[51] as discussed in section 2.3.1.

The anti-biofouling properties of certain polymers are popular among those pursuing *in vivo* applications since the formation of a protein corona can be detrimental to the function and stability of nanoparticles. Several groups have shown that PEG can reduce adsorption of BSA[38,87,88] and other proteins[70,89] to gold surfaces. When fibrinogen[90] and lysozyme[89] were found to induce aggregation of gold nanoparticles, coating nanoparticles with PEG prior to protein exposure reduced adsorption and prevented aggregation. Contrary to these results, some studies observed significant adsorption of BSA, regardless of PEG functionalization.[51] A thermokinetic study of BSA adsorption onto PEG, PAA, and PAH coated gold nanoparticles concluded that BSA adsorption occurs with all three coatings.[51] However, it was noted that the adsorption rate was slower for PEG- and PAA-AuNPs compared to PAH-AuNPs, presumably due to the net negative charge of BSA at pH 7[51]. Even in cases where PEGylation of AuNPs was shown to reduce protein adsorption, not all proteins were similarly affected. Strong adsorption of positively charged lysozyme to slightly negative PEG-AuNPs resulted in charge neutralization and in some cases induced aggregation.[87] While it is commonly believed that reducing

the amount of protein adsorption will benefit stability, the presence of free proteins in solution can also cause depletion-aggregation of nanoparticles decorated with ethylene glycols[38], without the need for direct surface adsorption. Given the mixed results of PEG, it is clear that these nanoparticle coatings do not provide a universal solution to particle stability against non-specific adsorption, especially in complex media containing multiple protein identities.

It should be noted that the presence of excess PEG in solution (not attached to the nanoparticle surface) can itself affect colloidal stability of gold nanoparticles via depletion stabilization[43]. Here, low molecular weight (Mw) PEG was found to promote depletion attraction (aggregation) while high Mw PEG promoted depletion repulsion (stabilization). This mechanism of stability is advantageous over polymer coating and protein corona stabilization since it leaves the surface free for attachment of other molecules[43]. However, free PEG may not have the same anti-biofouling properties as surface-attached PEG, and may not be as effective in preventing nanoparticle aggregation due to bridge flocculation.

2.4 Applications

A number of gold nanoparticle applications have arisen which may be sensitive to protein interactions. In some cases, unwanted protein fouling of nanoparticle surface could cause aggregation and prevent cellular uptake of therapeutic nanoparticles.[91] In other cases, the deposition of proteins on the surface could be used to enhance biocompatibility, increase colloidal stability, and increase circulation times.[92] Again others will be primarily concerned with how particles become aggregated or stabilized in solutions for protein sensing or diagnostic applications.[9–11,79] Here, we present some applications for which protein-nanoparticle interactions and colloidal stability are a concern, and address possible limitations.

2.4.1 Sensing and diagnostics

2.4.1.1 Conventional protein methods

Proteins play a vital role in countless biochemical and physiological processes. Variations in protein concentration or function can often be associated with ongoing biological process and overall health. Given their importance, the ability to detect and quantify proteins is a fundamental part of many bioanalytical and clinical investigations.[1,93,94] Conventional methods for protein quantification include the Bradford, bicinchoninic acid (BCA), and Lowry assays. These assays function based on the interaction between peptide bonds or aromatic residues in proteins with one or more chemical reagents to produce a colour change at a particular wavelength. The amount of colour change can then be used to estimate total protein concentration based on a standard curve. While these colorimetric assays are

relatively simple to perform, they cannot be used for protein identification since the response obtained is not specific to a given protein. The identification of proteins in solution is much more challenging than quantification. Gel-based assays such as polyacrylamide gel electrophoresis (PAGE) may provide an approximate size for a protein, but this alone cannot be used for conclusive identification since many polypeptides share similar molecular weights. Western blotting, enzyme-linked immunosorbent assays (ELISA), and protein microarrays can be used for protein identification, but only when paired with antibodies for the target of interest.[95] Furthermore, the lock-and-key model protein protein-antibody interaction necessitates that a probe be pre-selected for every analyte of interest. This, plus the difficulty and cost of obtaining target-specific probes can increase the complexity and cost of probe-based identification assays. Protein mass spectrometry is a powerful tool for identification but requires specialized training and expensive equipment. These factors make conventional methods impractical for the majority of point-of-care and consumer-level applications. The ideal protein assay would permit concurrent protein identification and quantification, while reducing overall cost and complexity.

2.4.1.2 Gold nanoparticle methods

The use of non-functionalized gold nanoparticles for colorimetric protein quantification was being explored as early as 1986, when it was demonstrated that the absorbance spectrum of colloidal gold undergoes red-shifting and peak broadening in response to BSA concentrations as low as 20 ng/mL (0.7 nM)[79]. Here, BSA solutions were incubated with commercially available colloidal gold nanoparticles and aggregation was monitored using characteristic changes in their absorption spectra. The main interfering factors identified by the author were variations between purified proteins, changes in solution pH, and the presence of surfactant (i.e. sodium dodecyl sulfate (SDS)). To avoid errors in quantification due to variation between proteins, the author recommended comparing samples to a protein standard containing the same species at known concentrations. The author also noted that this variation becomes less important with protein mixtures, where an averaging effect may occur, except in cases where one protein is dominant in a sample. The importance of solution pH supports the notion of electrostatic interaction between proteins and nanoparticles since changes in pH would affect the protein net charge, as discussed in section 2.3.1.1. Additionally, the presence of SDS likely impacts protein conformation and charge, thereby altering the response of colloidal gold. While not explicitly presented as sensing platforms, other studies have shown similar concentration-dependent responses which could be adapted to quantify protein concentration if paired with suitable protein standards.[33,38,96]

Aside from protein concentration, gold nanoparticles have also been used to quantify the degree of protein denaturation.[11] Here, citrate-stabilized gold nanoparticles were exposed to four globular proteins

(α-amylase, GFP, AMG, and BSA). Thermal denaturation of proteins prior to incubation with nanoparticles changed the observed peak response. Since transmission electron microscopy (TEM) confirmed that changes in absorption spectrum were a result of nanoparticle aggregation and not solely protein adsorption, the authors concluded that protein conformation could be determined by monitoring the degree of gold nanoparticle aggregation. The lower limits of detection ranged between 2 and 330 ng/mL (40 pM – 12 nM), while the upper limits ranged between 0.1 and 3.85 μg/mL (2-143 nM), depending on the protein identity and conformation. The effect of protein conformation on nanoparticle response was not uniform between the four proteins and the authors related these variations to the distribution of thiol groups, as discussed in section 2.3.2.2. Further studies by the same group used this method to determine the proportion of native and denatured proteins in a mixture.[97] While the distinguishing feature of this assay over conventional methods is the ability to discriminate between native and denatured proteins, care must be taken to ensure that protein denaturation does not lead to under- or over-estimation of protein concentration.

The quantification of individual proteins within the complex medium of a biological sample poses several difficulties. Most prominent of these are low concentrations of the target protein and the presence of many other interfering proteins. An investigation into detection of urinary lysozyme using anionic citrate-capped gold nanoparticles proposed a quantitative assay which leverages the high pI of lysozyme, relative to other proteins.[10] The authors suggest that positively charged lysozyme will bind preferentially to anionic gold nanoparticles, conferring some specificity to the assay. They also noted the relationship between solution pH and protein pI on nanoparticle aggregation, as discussed in section 2.3.1.1. Using gold nanoparticles to quantify lysozyme in aqueous solutions, the authors reported detection ranges between 10 and 60 nM which were also related to particle size (larger particles had higher detection limits). As with all the assays proposed thus far, variations in the adsorptive properties of lysozyme and other proteins on citrate-stabilized gold nanoparticles must be controlled to ensure repeatable aggregation behavior.

Nanoparticle aggregates can also be used for surface-enhanced Raman spectroscopy (SERS). The locations at which two separate nanoparticles touch are functionally similar to spiky gold nanoparticles which enhance electromagnetic fields, leading to a stronger Raman signal.[98,99] One application of gold nanoparticle aggregates for SERS was demonstrated by Jung et al.[98]. Here, pH sensitive "SMART" gold nanoparticles aggregate following uptake by cancer cells and showed distinct Raman peaks from the nanoparticle surface. While aggregation is beneficial for this strategy of Raman surface enhancement, sub-nanometer gaps are critical for maximum SERS enhancement[99] and it is possible that thick protein coronas could keep particles far enough apart to reduce this effect.

Given that viral capsid is composed of proteins, it is possible that developments in protein-nanoparticle interactions can be expanded to applications in viral sensing and analysis. The binding ratio between gold nanoparticles and viruses will depend on their relative size, but the comparable size of nanoparticles and viruses presents an interesting question of whether nanoparticles will aggregate given the limited number of surface interactions possible. One potential aggregation mechanism, similar to that previously identified [81] would be inter-particle bridge formation between individual particles and whole viruses. Alternatively, individual proteins may interact with gold nanoparticle if the viral capsid is disassembled.

2.4.2 Therapeutics

Photothermal therapy (PTT) is being heavily investigated as a method for cancer treatment. In brief, nanomaterials capable of converting near-infrared (IR) radiation into heat accumulate in tumors and are irradiated to generate localized hyperthermia which kills or damages cells. Gold nanoparticles are among the most promising PTT materials.[100] Their size and aspect ratio can be controlled to tune absorbance to the "tissue optical window" of 650-1350 nm where light can penetrate deep into tissue while maintaining dimensions that permit uptake by cells.[101] Aggregation of gold nanoparticles prior to accumulation in tumors could reduce this effect and shorten circulation times since nanoparticle size strongly influences clearing rates.[102] Instead of tuning individual particle size and shape for increased uptake and near-IR heating, small gold nanoparticles can also be used which form large aggregates upon cellular uptake, shifting their absorbance to the near-IR region by plasmon coupling.[103] For instance, nanoparticles have been coated with pH-responsive molecules which aggregate by adopting positive and negative charges under the mildly acidic intracellular conditions.[98,104] As in the first strategy, extracellular aggregation may hinder uptake by cancer cells and must be avoided. However, this method relies on particles to aggregate once inside tumor cells. In the event that adsorption of proteins produces a stabilizing corona and prevents electrostatic aggregation, plasmon coupling will not occur and photothermal efficiency will diminish.

Finally, gold nanoparticle-protein aggregates have also been proposed for drug-delivery. In one study, lysozyme was used to induce aggregation of citrate-stabilized gold nanoparticles and form large protein-nanoparticle complexes.[105] These complexes were then loaded with a hydrophobic or hydrophilic drug. BSA was used to stabilize the protein-nanoparticle complexes by forming an external stabilizing layer. This application is particularly interesting with regards to protein adsorption and colloidal stability since it uses proteins for both destabilization (formation of drug-carrying agglomerates) and stabilization (to prevent further aggregation of these complexes *in vivo*). Lysozyme

is a clear choice for forming gold nanoparticle aggregates since it has a pI near 11, rendering it positively charged at physiological pH, and several groups have observed lysozyme-induced aggregation of negatively charged gold[10,89] and silica nanoparticles[81]. The adsorption of BSA was also noted by the authors as benefiting not only the stability of drug carrying agglomerates, but also improving carrier uptake by cancer cells.[105]

2.5 Conclusion

The colloidal stability of gold nanoparticles is a fundamental consideration for nanotechnology applications. Many virtues of nanoparticles are directly related to their aggregation state. Despite extensive research in the field, there is much room for improvement in our ability to predict and control nanoparticle aggregation. For many biological samples, non-specific nanoparticle-protein interactions remain the crux of this issue as these interactions have proven to be highly multifaceted. In most cases, the aggregation or stability of gold nanoparticles is determined by numerous interacting factors such as medium ionic strength, pH, protein charge, nanoparticle charge, protein structure, and surfactant concentration. It is therefore important to consider the complex interactions between these factors when designing gold nanoparticle applications for *in vivo* and *in vitro* applications.

In this review we have outlined several key factors which have been shown to affect gold nanoparticle-protein interactions and their resultant effect on colloidal stability. We have also shown how these factors may become interrelated in their effects. By this method, we have highlighted the complexity with which proteins and gold nanoparticles interact. Unfortunately, this complexity is not fully appreciated by many articles in the field. This hinders the development of gold nanoparticles for point-of-care or field use. By acknowledging these factors, we can begin to reconcile contradictions over nanoparticle behavior, thereby furthering the potential of gold nanoparticles in biological applications.

Chapter 3

"Chemical nose" biosensor for detecting proteins in complex mixtures

3.1 Summary

A growing understanding of the fundamental role of proteins in diseases has advanced the development of quantitative protein assays in the medical field. Conventional techniques for protein analysis include ELISA, western blotting, mass spectrometry and various quantitative assays (e.g. Bradford, Lowry, BCA). However, many of these conventional strategies require specialized training, expensive antibodies, or sophisticated equipment, raising assay costs and limiting their application to laboratory analysis. Here, we present the application of a "chemical nose" type colorimetric gold nanoparticle sensor for detection, quantification, and identification of single proteins, protein mixtures, and proteins within the complex environment of human serum. The unique interactions between a mixture of two different gold nanoparticle morphologies (spherical and branched) and six separate proteins (bovine serum albumin, human serum albumin, immunoglobulin G, fibrinogen, lysozyme, and hemoglobin) generated distinguishable protein- and concentration-dependent absorption spectra, even at nanomolar concentrations. Furthermore, we show that this response is sensitive to the relative abundance of different proteins in solution, permitting analysis of protein mixtures. Finally, we demonstrate the ability to distinguish human serum samples with and without a clinically relevant two-fold increase in immunoglobulin G, without the use of expensive reagents or complicated sample processing.

3.2 Introduction

Protein detection, identification, and quantification assays have diverse applications ranging from biomedical diagnostics and health monitoring[107,94,93], to environmental[108,109] and consumer protection[110,111]. While several methods for protein identification are commercially available, many conventional methods such as ELISA are not well-suited for consumer level or point-of-care applications due to procedural complexity, equipment requirements, or high assay cost. Furthermore, these assays generally rely on "lock and key" models for protein detection, whereby a specific antibody is required to detect a protein of interest and detection of multiple proteins requires several antibodies. The detection of multiple analytes simultaneously, commonly referred to as multiplexing, allows for more complete analysis of biological samples. However, multiplexed protein analysis often employs several probes (e.g. protein microarray)[112] or specialized equipment such as mass spectrometers[94].

Increasing accessibility of multiplexed protein analysis will require the development of new biosensing techniques that lower cost and equipment requirements. Colorimetric nanosensor platforms are increasingly studied for biosensing applications in research, clinical, and consumer level environments due to their ease-of-use, and high sensitivity.[3,52,113] Among these platforms, gold nanoparticles are popular due to their unique optical properties.[114,115] As particle size increases, or particles aggregate in solution, their electromagnetic absorption peak shifts to longer wavelengths.[4,57,116] Since the peak wavelengths for gold nanoparticles typically fall within the visible range of the electromagnetic spectrum, these shifts can be perceived as changes in color without specialized equipment.

One common method for protein detection using gold nanoparticles is to functionalize them with target-specific probes such as antibodies, peptides, or aptamers. These surface-bound molecules can then bind to freely diffusing proteins, thereby forming inter-particle bridges and producing a colorimetric response. However, this "lock and key" strategy for detecting proteins suffers from similar limitations to conventional methods. As a result, probe-functionalized gold nanoparticles are not optimal for low-cost broad-spectrum protein analysis. Another strategy relies on the displacement of a fluorophore from the gold nanoparticle by a target analyte.[117] In this case, analyte presence is monitored by changes in fluorescence rather than absorbance. An array of nanoparticles with different surface modifications and protein interactions can be used to establish an identifying fingerprint, but the need for fluorophores and fluorescence measurements raises manufacturing and equipment requirements.

While certain strategies use probes for protein-specific binding, it is also well known that protein adsorption can occur non-specifically on the surface of both metallic and non-metallic nanoparticles[81,90,118]. The collection of proteins adsorbed onto the surface of these nanoparticles is known as the protein corona and has been shown to affect stability of nanoparticle solutions. For instance, some studies suggest that adhesion of proteins onto gold nanoparticles can increase their stability and may prevent *in vivo* aggregation.[76,88] Other studies show that the presence of certain proteins can destabilize nanoparticle solutions.[11,81,89] Furthermore, the degree of protein coverage and particle stability is often related to protein concentration.[31,81] While the effect of protein adsorption and corona formation on nanoparticle stability is commonly studied due to its impact on diagnostic and therapeutic platforms, few studies have investigated how these non-specific interactions can be used for protein identification and sensing.[9–11,79]

In a "chemical nose" system, several different responses to a single analyte are used to construct a unique fingerprint for that analyte, thereby improving distinction over a single-response system. This

has been previously demonstrated for detection of bacteria using gold nanoparticles.[119] Since nanoparticle morphology plays a key role in protein-nanoparticle aggregation, the response of different shapes can also be used in a "chemical nose" for improved distinction between proteins. In this study, we show that branched and spherical CTAB-coated gold nanoparticles produce unique colorimetric responses to different proteins, and that a 1:1 (v:v) mixture of the two (from now on, referred to as "chemical nose" solution) can be used to discriminate between six proteins: bovine serum albumin (BSA), human serum albumin (HSA), immunoglobulin G (IgG), lysozyme (Lyz), fibrinogen (Fib), and hemoglobin (Hgb). We also demonstrate how relative abundance of proteins in a binary mixture can be determined based on this response. Finally, we use this platform to detect elevated globulin levels in human serum, which can serve as an indication of disease status and predictor of mortality in cancer patients[2,120–124].

3.3 Materials and Methods

3.3.1 Materials

Gold (III) chloride hydrate (HAuCl$_4$·xH$_2$O), cetyltrimethylammonium bromide (CTAB), sodium borohydride, silver nitrate, hydrochloric acid, nitric acid, sodium hydroxide, L-ascorbic acid, bovine serum albumin (A2153), albumin from human serum (A1653), IgG from human serum (I4506), fibrinogen from human plasma (F3879), lysozyme from chicken egg white (L6876), human hemoglobin (H7379), and human serum (H4522) were purchased from Sigma-Aldrich (Oakville, ON, Canada). Trisodium citrate dihydrate and BupH phosphate buffered saline packs were purchased from Thermo Fisher Scientific (Burlington, ON, Canada). Sterile UV-star 96-well microplates, scintillation vials (20 mL), sodium chloride (ACS grade), Nalgene sterilization filter units (0.2 µm pore size), 15 mL polypropylene centrifuge tubes, and 1.7 mL polypropylene microcentrifuge tubes were purchase from VWR (Mississauga, ON, Canada). 400 mesh formvar/carbon coated copper grids were purchased from Canemco Inc (Gore, QC, Canada). All procured chemicals were used without further purification. The 20 mL vials used for gold nanoseed synthesis were cleaned using 12M sodium hydroxide and larger glassware was cleaned using aqua regia as described in a previously published protocol[125]. Water used for the preparation of solutions was purified using a Millipore water filtration system to an electrical resistivity greater than 15 MΩ·cm.

3.3.2 Synthesis of gold nanoparticles

CTAB-coated gold nanoparticles were synthesized according to a previously published protocol[65]. All synthesis solutions were prepared in Millipore water (>15 MΩ·cm). Briefly, gold seed precursor was prepared by adding 60 µL of ice-cold sodium borohydride to a solution containing 18.812 mL of

Millipore water, 188 µL of 10 mg/mL gold (III) chloride, and 1 mL of 2 mM trisodium citrate under vigorous stirring. Following addition of sodium borohydride, the solution was stirred for 1 minute and left to mature overnight under dark ambient conditions. Nanoparticle growth solution (221.76 mL) was prepared under moderate stirring by adding 8.974 mL of 11 mM gold chloride, 1.344 mL of 5 mM silver nitrate, and 1.442 mL of 100 mM L-ascorbic acid to 210 mL of either 1.47 mM or 7.33 mM CTAB (for spherical (red) and branched (blue) nanoparticles respectively). Finally, 5.6 mL or 2.24 mL of gold seed precursor (for spherical (red) and branched (blue) nanoparticles respectively) was added to the nanoparticle growth solution, and stirred for an additional 1.5 minutes, at which point the solution was incubated overnight under dark ambient conditions. The final nanoparticle solution was pelleted via centrifugation (16000 RCF for 15 minutes) and resuspended in 1 mM CTAB solution.

3.3.3 Protein solutions

Prior to reconstitution of lyophilized proteins, BSA, HSA, IgG, fibrinogen, lysozyme, and hemoglobin were stored at -5 ^{o}C or -20°C, as per supplier's recommendation. Fresh protein solutions were prepared prior to each experiment. Solutions were prepared by weighing out the appropriate amounts of protein into a microcentrifuge tube, and reconstituting in a calculated volume of purified water, sterile saline, or sterile phosphate-buffered saline (PBS), to the desired final concentration. Lower ionic strength saline and PBS (1/4X and 1/16X) were prepared by diluting stock (1X) NaCl and PBS solutions (I = 450 mM) in Millipore H$_2$O at 1:3 or 1:15 ratios. After reconstitution, protein concentrations were adjusted by measuring absorbance at 280 nm (A280) using an Epoch^{TM} Microplate Spectrophotometer. Molar concentrations were determined using the Beer-Lambert Law:

$$A = \varepsilon \times l \times c \qquad \text{(Eq. 3.1)}$$

where A is the optical density (OD) of the sample, ε is the molar absorption coefficient of the protein obtained from the supplier or literature (Table 3.1), l is the optical path length, and c is the molar concentration of the protein solution.

Table 3.1 Physical and optical parameters of proteins used for concentration determination. Adapted from Moyano et al.[117]

Protein	Mw	E_{280} $(10^3/M^{-1}cm^{-1})$	A280 $(4.5 \mu M)$	Reference
BSA	66.4	44.3	0.199	Sigma-Aldrich
HSA	66.5	35.3	0.159	Sigma-Aldrich
IgG	150	210	0.945	Moyano 2011
Fib	340	513	2.310	Sigma-Aldrich
Lyz	14.3	37.8	0.170	Moyano 2011
Hgb	64.5	130	0.585	Sigma-Aldrich

Serial dilutions were performed to obtain solutions varying in concentration from 450 μM to 27.5 nM. After adding 200 μL of gold nanoparticle solution to 100 μL of each protein sample, the final protein concentrations were one third the normalized concentration, such that final solutions ranged from 150 μM to 9.2 nM. Final concentrations following dilution in the 96-well plate were confirmed by adding 200 μL of Millipore H_2O to 100 μL of the respective protein dilution, and measuring absorbance at 280 nm. Due to limitations in A280 quantification, protein concentrations were calculated directly from absorbances where absorbance was in the linear range of the spectrophotometer (0.1-2.0), and extrapolated for samples beyond this range. Protein concentrations presented in the results and discussion section represent molar concentrations following the 1/3 dilution, as determined using A280. For protein identification assays, protein solutions were adjusted to a final concentration of 4.5 μM using A280 (Table 3.1), and diluted 1/10 in 1/4X PBS for a final concentration of 450 nM. After adding 200 μL of gold nanoparticle solution to 100 μL of each protein identification sample, the final protein concentration was 150 nM. For mixtures of HSA and IgG, individual protein concentrations were first adjusted to 450 nM as previously describes, then mixed by volume to obtain the desired mole fractions of HSA and IgG such that the total protein concentration following addition of nanoparticles was 150 nM.

3.3.4 Serum preparation with IgG

Human serum samples for baseline IgG levels were diluted 20X in 1/4X PBS without any added protein. Serum samples for elevated IgG levels were diluted 20X in 1/4X PBS containing 3.42 μM IgG. The resultant IgG concentrations prior to incubation with gold nanoparticles were approximately 3.25 μM for baseline serum (based on average IgG concentrations for human adult males) and 6.5 μM for high IgG serum, a two-fold increase assuming a mean total IgG concentration of 65 μM in healthy adult males[126].

3.3.5 Protein-gold incubation

Concentration-dependent response, protein identification, and serum experiments were assessed spectrophotometrically in a transparent 96-well plate. 100 μL of each protein sample or solvent control was added to the 96-well plate. Triplicate samples for each dilution were used for concentration-dependent response, and eight replicates were used for identification and serum tests. 200 μL of the gold nanoparticle solution was then added to each well containing protein or control solution. Plates were then placed on a Stovall Belly Dancer orbital shaker (Peosta, IA, USA) for 2 minutes prior to 20 hour incubation in the dark at room temperature. Following incubation, an Epoch™ Microplate Spectrophotometer (Winooski, VT, USA) was used to obtain spectral scans for each well containing gold nanoparticles. Spectra were collected from 300-999 nm wavelengths, in increments of 1 nm.

3.3.6 Quantifying gold nanoparticle response

The extent of gold nanoparticle aggregation was quantified by monitoring changes in peak absorbance relative to the solvent control. First, the position of the absorbance peak for the 1/4X PBS control (1° peak in wavelength nanometers) was determined from control spectral scans. Absorbance values at the 1° peak position were then noted for samples containing protein. Baseline absorbance at 800 nm was then determined for each sample. Peak height was calculated by subtracting each sample's baseline absorbance (800 nm) from the sample's absorbance at the 1° peak position:

$$height_{sample} = A_{sample}(1^o\ peak\ position) - A_{sample}(800\ nm) \qquad (Eq.\ 3.2)$$

Peak heights were then normalized against the control to obtain a normalized response for each protein sample:

$$Normalized\ sample\ response = height_{control} - height_{sample} \qquad (Eq.\ 3.3)$$

Statistical significance between peak heights for baseline and elevated IgG serum samples was determined using Microsoft Excel® via an independent two-tailed heteroscedastic t-test. A heteroscedastic t-test was used due to unequal variances in the baseline and elevated samples.

3.3.7 Protein classification

Principal Component Analysis (PCA) was conducted using MATLAB®. Protein solutions were grouped based on the resultant gold nanoparticle absorbance spectrum. Due to the broad extent of spectral shifts observed during protein-induced aggregation, all 700 wavelengths of the spectrum (300-999 nm) were used for classification. Confidence ellipses (95%) were also calculated using MATLAB®.

3.3.8 Transmission electron microscopy

Gold nanoparticle sizes and shapes were confirmed using a Phillips (Eindhoven, The Netherlands) CM10 TEM. Copper TEM grids (400 mesh formvar/carbon coated) were prepared under ambient conditions by overnight evaporation of a 5 μL droplet of gold nanoparticle solution directly onto a grid. TEM micrographs were analyzed using ImageJ.

3.4 Results and Discussion

3.4.1 Ionic strength

The majority of protein detection and identification experiments are performed in aqueous solutions. Since it has been shown that ions can mediate both the colloidal stability of gold nanoparticles in solution[35,127], as well as the electrostatic interaction between proteins and gold nanoparticles[51], it was important to choose a salt concentration which would maximize the performance of our assay. In the absence of proteins, high salt concentrations can be used to destabilize gold nanoparticles.[43,44] With proteins in solution, the ionic composition of a medium can affect both protein-protein interactions[128] and protein adsorption on surfaces[29]. To determine the optimal ionic concentration for protein-induced "chemical nose" aggregation, serial dilutions of BSA were prepared in deionized water, saline (NaCl), or PBS at varying salt concentrations, such that the final ionic strengths of NaCl and PBS were 450, 112.5, or 28.125 μM (from now on referred to as 1X, 1/4X, and 1/16X, respectively). These concentrations were chosen since they are below the experimentally observed salt concentration which causes gold nanoparticle aggregation. The results are shown in Figure 3.1.
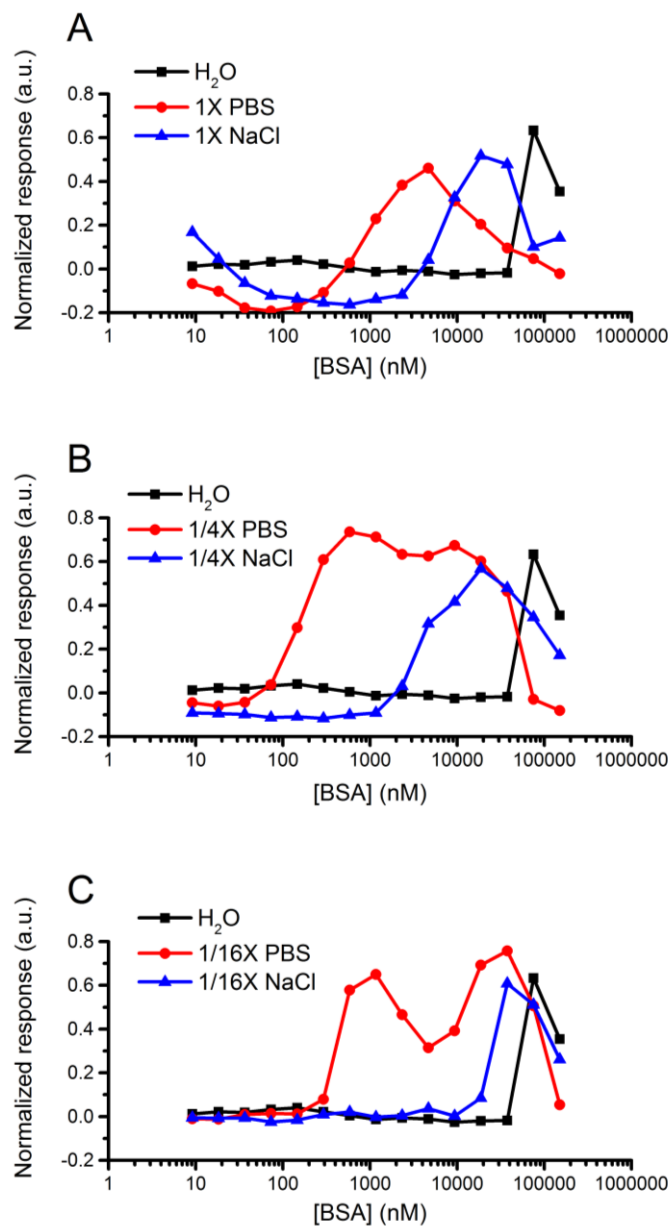
Figure 3.1 Concentration-dependent aggregation of "chemical nose" nanoparticles to BSA solutions of different ionic strength and composition.

In all observed cases, protein solutions dissolved in PBS induced nanoparticle aggregation at lower protein concentrations than those dissolved in NaCl with the same ionic strength (Figure 3.1). This suggests that polyionic species (e.g. phosphate groups in PBS) have a larger effect on mediating nanoparticle aggregation. The increase in aggregation at lower protein concentrations is favourable for high sensitivity detection assays. Additionally, solutions of 1/4X NaCl and 1/4X PBS outperformed their higher and lower ionic strength counterparts, while pure deionized Millipore H_2O was the least

sensitive. These findings suggest the existence of an optimal ionic environment which facilitates protein-induced nanoparticle aggregation. For optimal performance at low concentrations, subsequent experiments were performed by diluting protein and/or serum in 1/4X PBS.

3.4.2 Shape-dependent response

In order to have good distinction between proteins, it is necessary to obtain several unique responses to the same analyte. The proteins can then be identified based on the unique pattern or fingerprint of responses. One simple method for changing the response of gold nanoparticles is to change their morphology. By changing gold nanoparticle shape (i.e. from spherical to branched) we can alter their optical absorbance spectra and how they interact with their environment. This technique has been previously demonstrated only for the detection of bacteria.[65,119,129]

It should be noted that variations in nanoparticle synthesis procedures can affect nanoparticle morphology, resulting in slight variations of size, surface features, edge angles, or overall shape. Given the potential effect of morphology on gold nanoparticle-protein interactions, variability in gold nanoparticle shapes could lead to different responses. However, repeated studies using the above-mentioned synthesis procedure have optimized shape-control of branched and spherical nanoparticles with respect to both particle size and degree of branching [65,129]. Previous statistical analysis of particles produced by this method has shown that the configuration of seed and surfactant used in this study yields a small distribution of spherical particles with diamaters of approximately 32 nm, and consistent branched particles with approximate diameters of 60 nm and an average of 5.5 branches which are on average 9 nm long [65]. The spectrophotometric profiles of nanoparticles used in the current study also match those collected previously. This optimization allows for repeated synthesis of nanoparticles with minimal variation in morphology or optical properties between batches. Furthermore, the crystalline structure of gold nanoparticles is an important consideration for protein-nanoparticle interactions since it can define overall particle morphology following nanoparticle growth. In the previously described method, silver ions are deposited onto gold nanoseed by underpotential deposition (UPD)[65]. These ions then create active sites for nanoparticle branch formation. Since underpotential deposition favours certain crystal facets[130], the crystalline structure will influence active site formation and, by extension, branch orientation which could ultimately affect the protein-nanoparticle interaction.

Here, we have optimized the detection conditions to get a differential response in the presence of different proteins. To determine whether these two nanoparticle morphologies respond differently to proteins, we incubated branched (Figure 3.2A), spherical (Figure 3.2B), and a 1:1 mixture of both with BSA, IgG, and a protein-free medium (1/4X PBS). At a concentration of 150 nM, both BSA and IgG

induced nanoparticle aggregation, as evidenced by decreases in absorbance intensity, red-shifting of the spectrum, and broadening of the absorption peak (Figure 3.3).
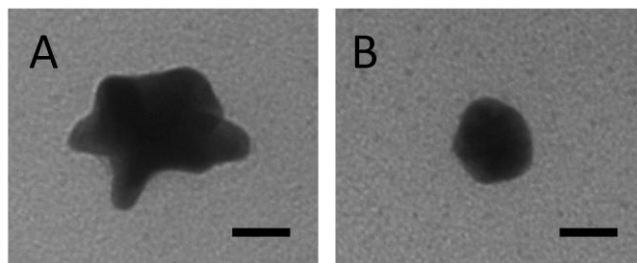
Figure 3.2 TEM micrographs of A) branched (blue) and B) spherical (red) nanoparticles. Scale bars represent 20 nm.

A difference in response between spherical and branched morphologies was also apparent. While the absorbance peak for branched nanoparticles was completely flattened in the presence of both BSA and IgG, BSA only induced partial flattening in spherical nanoparticles (Figure 3.3B) whereas IgG induced complete flattening (Figure 3.3C). For both proteins and the negative control, the absorbance of the "chemical nose" solution has features resembling both spherical (red) and branched (blue) curves, suggesting that both nanoparticle morphologies contribute to the final spectrum when mixed together. When two or more nanoparticles are combined together with drastically different peak absorbance wavelengths, then it may be possible to observe both maxima in the combined solution. In this way, aggregation of both particles might be monitored independently based on absorbance at their corresponding wavelengths. The combination of two or more nanoparticle morphologies in this way can provide added discriminatory power from a single sample well, thereby simplifying the assay.[129]
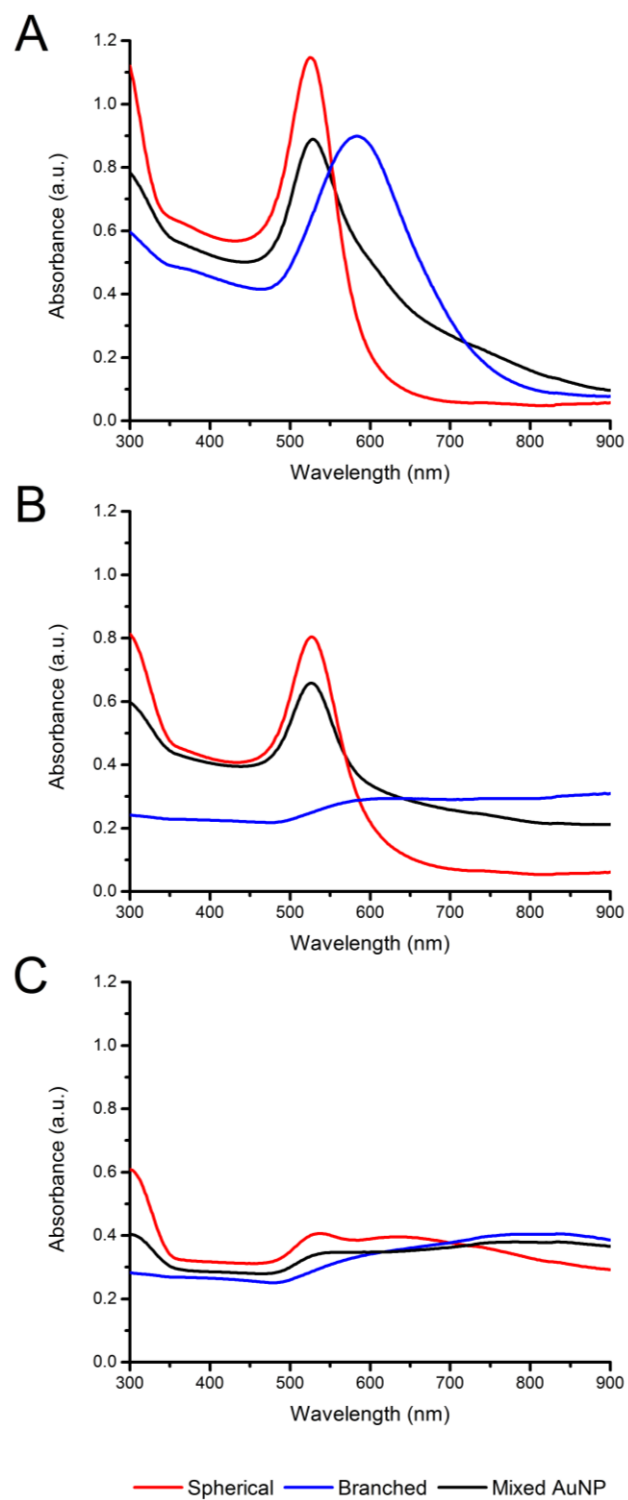
Figure 3.3 Absorbance spectra for spherical, branched, and mixed (spherical and branched, 1:1 by volume) nanoparticle solutions when incubated with A) PBS, B) 150 nM BSA, or C) 150 nM IgG. Average curves are shown (n = 8).

3.4.3 Concentration-dependent response

Several investigations have observed concentration-dependent effects of proteins on gold nanoparticle aggregation and adsorption.[11,79] Despite extensive interest in the field, many confounding factors make characterizing the aggregation mechanisms difficult. Observed effects can be influenced by protein identity[69], protein concentration[11], nanoparticle coatings (e.g. PEGylated surfaces[89], citrate-stabilization or CTAB-stabilization[40,76]), medium (e.g. DI H_2O, PBS[40], NaCl[88], citrate[76]), and experimental set-up[11,81]. To determine the concentration-dependent aggregation of CTAB-coated gold nanoparticles to the proteins in this study, fifteen 2X serial dilutions were prepared for each protein in 1/4X PBS. The resulting protein concentrations ranged from 450 µM to 27.46 nM (BSA, HSA, Lyz, Hgb) and from 28.125 µM to 1.72 nM (IgG, Fib). Lower concentrations of IgG and Fib were used due to preliminary results, which showed higher response for these proteins. By combining these solutions (100 µL) with gold nanoparticles (200 µL) in a 96-well plate, the final protein concentrations were further diluted to one third of these values. A negative control containing only 1/4X PBS serves as a baseline for comparison. Within 1 minute of nanoparticle addition, several protein dilutions displayed a visible change in color when compared to the negative control. This color change progressed rapidly for the first 10 minutes of incubation. To allow sufficient time for assay color to stabilize, samples were incubated for 20 hours under dark ambient conditions. Figure 3.4 shows the resulting aggregation response curves, presented as a peak-height difference between sample and control.
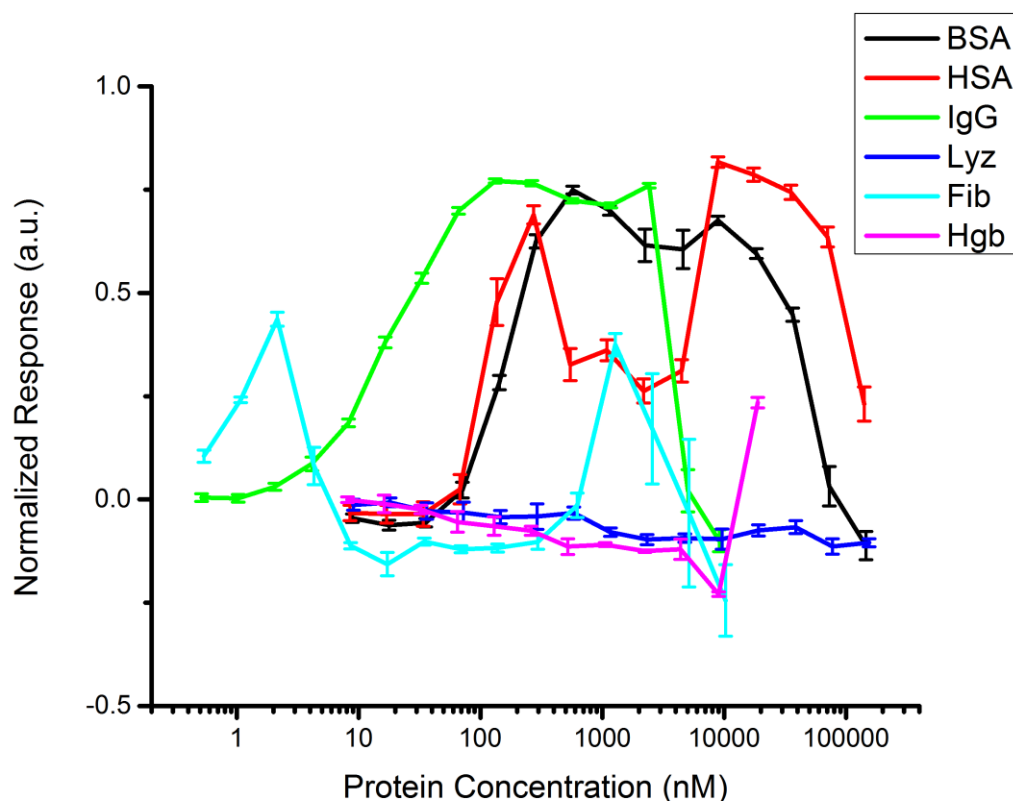
Figure 3.4 Concentration-dependent aggregation of CTAB-stabilized "chemical nose" to different proteins. Higher normalized response, defined as the difference in absorbance peak height between sample and control, indicates more aggregation. Mean response values (n=3) are presented ± S.D.

Each protein exhibits a unique concentration-depending aggregation curve. Furthermore, while BSA and HSA share similar structures, isoelectric points, and 76% amino acid sequence identity, their response curves are clearly distinguishable. While some proteins (BSA, HSA, IgG) lead to significant change in absorbance over a wide range of concentrations (73 μM to 5 nM), others respond only at certain concentrations (Fib, Hgb), while the remainder produce little to no response (Lyz). The bell-shaped response common to BSA, HSA, and IgG suggests the existence of different aggregation regimes for high, moderate, and low protein concentrations. Previous studies have described similar bell-shaped response curves when exposing negatively-charged polystyrene and PMMA nanoparticles to IgG.[81] The authors of this study proposed that high protein concentrations saturate the particle surface, reducing the overall aggregate size, while intermediate concentrations allow for aggregation by bridge formation where a single protein can bind to more than one nanoparticle. Other studies showed that progressive addition of BSA to a citrate-stabilized AuNP solution leads to an increase in

aggregation up to a saturation point beyond which no more aggregation occurred.[11] It is likely that the bell-shaped response was not observed by this group since protein concentration was steadily increased and irreversible particle aggregation occurred before the surface was saturated with protein. In this parallel comparison of several different proteins under identical conditions, we were able to discern varying ranges of aggregation and sensitivity.

3.4.4 Protein Identification

The ability to distinguish between different proteins is another valuable aspect of broad-spectrum biomolecular sensing. A multiplexed system of functionalized gold nanoparticles where different nanoparticles bind to different targets has been proposed[131], but the requirement to have one nanoparticle per protein limits the variety of proteins which can be identified. To assess the potential for protein discrimination at nanomolar concentrations using non-specific gold nanoparticle solutions, we prepared six protein solutions and normalized their concentration to 450 nM using absorbance at 280 nm. Each protein was then incubated with the "chemical nose" solution such that the final protein concentration was 150 nM. Within 1 minute of gold nanoparticle addition, BSA, HSA, and IgG were noticeably different in appearance than the 1/4X PBS control. The differences between Fib, Lyz, Hgb, and control were less noticeable. Even after 20 hours of incubation, these samples were not appreciably different to the unaided eye. Following incubation, full spectral scans revealed protein-dependent variations in absorption spectra. Average absorption curves for each protein are plotted in Figure 3.5A and show the difference between equimolar solutions. The contour plot in Figure 3.5B highlights sample-to-sample similarity of the 6 proteins, where the horizontal layers within each plot represent 8 replicates. PCA classification of these spectra established that the first two principal components could account for 98.7% of the observe variability. A biplot of PCA scores in Figure 3.6 shows the grouping of samples based on their protein identity. While large separation was observed for those proteins producing a visually noticeable response (BSA, HSA, and IgG), even those solutions which were not appreciably different by eye (i.e. Fib, Lyz, Hgb) could be resolved using PCA classification (Figure 3.6).

38
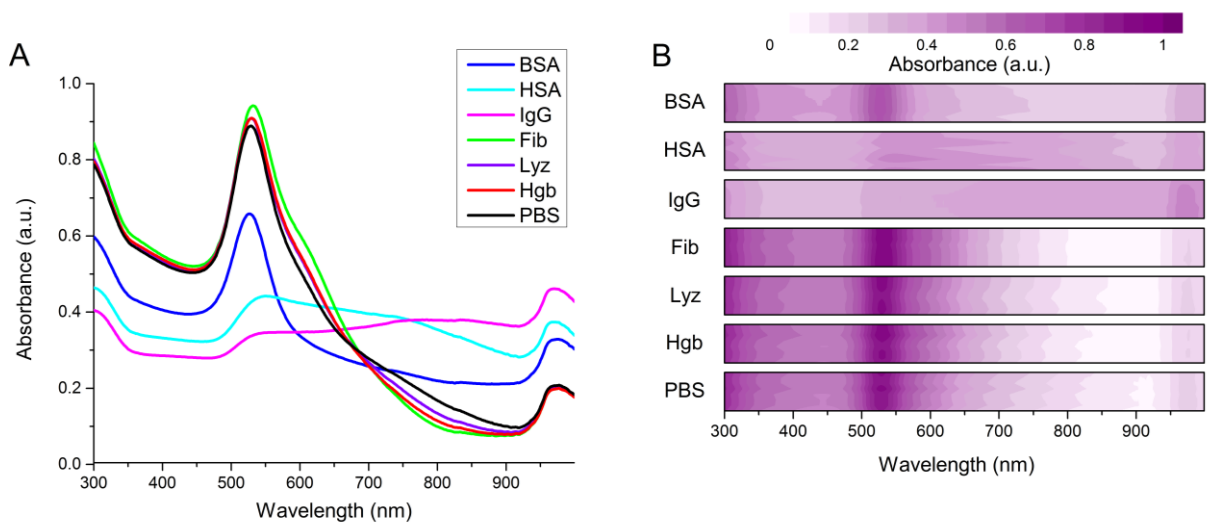
Figure 3.5 Absorption spectra for "chemical nose" solutions with 6 different protein samples at 150 nM. A) Average absorption curves (n = 7 or 8) highlight differences between proteins. B) Contour plots of individual absorption curves (n = 7 or 8) highlighting similarity between replicates.
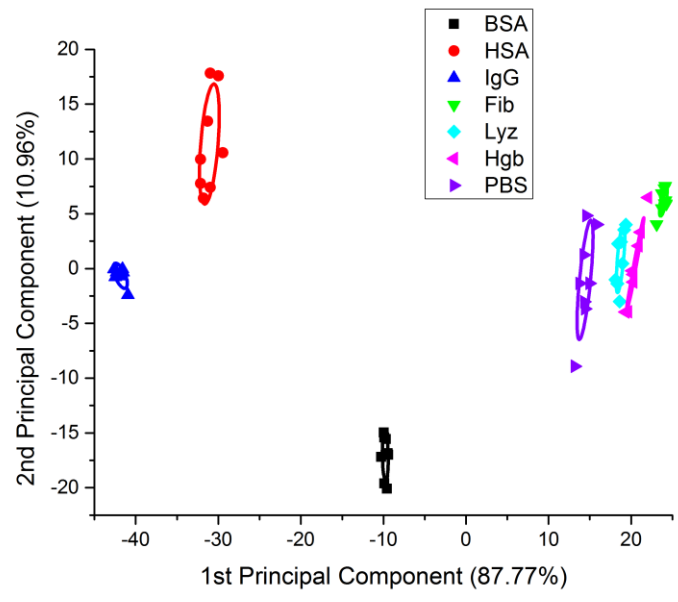
Figure 3.6 Principal Component Analysis (PCA) biplot of "chemical nose" response to different proteins at 150 nM. Ellipses represent 95% mean confidence levels.

3.4.5 Protein Mixtures

While the detection and quantification of single proteins is often useful in research environments, many samples may contain mixtures of proteins. In particular, clinical samples used for diagnostics will almost certainly contain a variety of different proteins and components. The "chemical nose" solution was combined with binary mixtures of HSA and IgG to determine whether their relative abundance affects the observed response. For each mixture, the total protein concentration was held constant at 150 nM and the mole fraction of HSA was set to 75%, 50%, or 25%. These samples were also compared to the single protein solutions containing 150 nM HSA and 150 nM IgG. As is shown in the resulting PCA biplot (Figure 3.7), samples containing only HSA or IgG form two separate clusters, while mixtures fall in between the two. This suggests that the absorption spectra for binary mixtures of HSA and IgG contain features of both pure solutions. It is interesting to note that while the clusters for mixed samples fall between HSA and IgG, they are not evenly spaced as may be expected if both proteins were contributing equally to the response. In fact, 25% and 50% HSA lie closer to IgG than HSA, and 75% HSA falls near the midpoint between the two populations. This is likely due to the fact that 150 nM IgG has a stronger aggregating effect compared to 150 nM HSA (Figures 3.4 and 3.5).
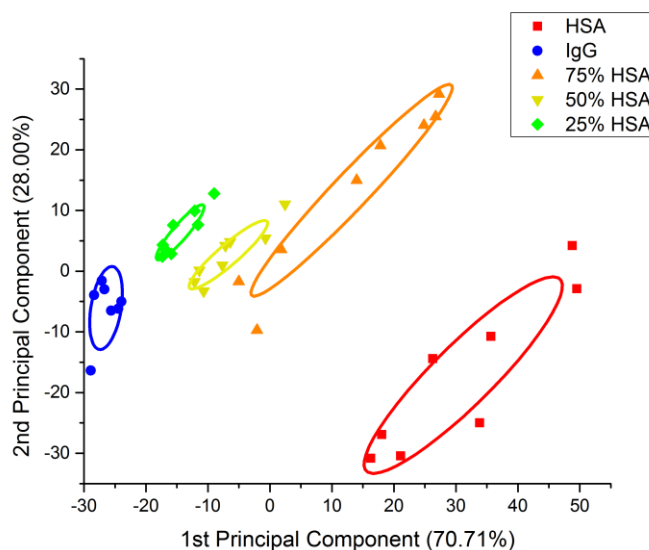
Figure 3.7 Principal Component Analysis (PCA) plot of "chemical nose" response to different mixtures of proteins. Composition reflects mole fraction of HSA in 150 nM total protein (HSA + IgG) concentration. Ellipses represent 95% mean confidence levels.

3.4.6 Complex Media

The quantification of protein levels in complex media such as serum can be used to diagnose a multitude of diseases.[2,94,120] Total protein and albumin/globulin ratio (AGR) are among the routine tests ordered by health care providers in determining a patient's health status. In particular, low pretreatment AGR is often associated with increased mortality in cancer patients and may be a valuable predictor of therapeutic success.[121–124] A serum IgG level greater than 1.5 times the upper normal limit is also one of the primary diagnostic criteria for autoimmune hepatitis[2]. The "chemical nose" system could be trained to distinguish between samples containing various levels and ratios of protein commonly found in serum. To obtain serum samples with elevated globulins, normal adult male serum was diluted in 1/4X PBS containing human IgG. Normal serum was then diluted in the same volume of 1/4X PBS without IgG to serve as a baseline comparison. The concentrations of IgG chosen for elevated and baseline samples were based on average IgG levels in healthy adult males[126] and represent an approximate two-fold increase. Diluted serum samples containing elevated or baseline IgG levels were then mixed with the "chemical nose" solution. The resulting average absorption curves for 8 replicates are shown in Figure 3.8A. The vertical shift in curve position relative to the 1/4X PBS control indicates that overall absorbance was significantly higher, likely due to slight sample turbidity. However, when normalized against a baseline absorbance at 800 nm, a two-tailed t-test reveals that peak height for serum samples containing elevated IgG was significantly lower compared to the baseline serum sample ($p<0.01$). The PCA biplot in Figure 3.8B demonstrates the separation of both groups based on the features of their absorbance spectra.
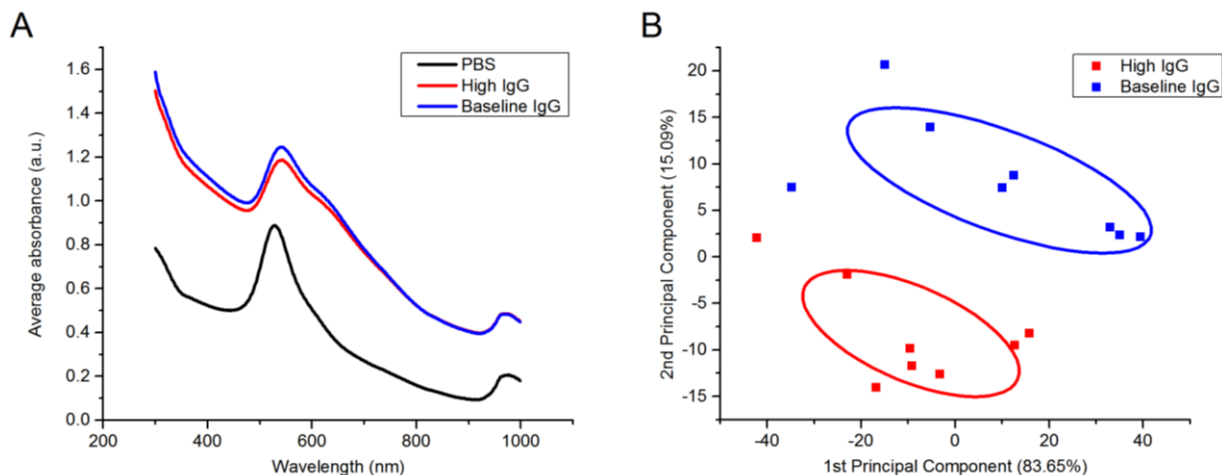
Figure 3.8 A) Mean absorption spectra for "chemical nose" solutions with serum containing baseline and high IgG (n = 8). B) Principal Component Analysis (PCA) plot of "chemical nose" response to serum containing high and baseline IgG. Ellipses represent 95% mean confidence levels. The observed decrease in peak height between baseline and high IgG was statistically significant at $p < 0.01$.

3.5 Conclusion

We demonstrated that the differential effect of various proteins on gold nanoparticle absorption spectra can be used to detect, identify, and quantify proteins in aqueous solutions, mixtures, and complex media such as human serum. We also noted the effect of ionic strength on this response and optimized the conditions for detection of nanomolar protein concentrations. Variations in the concentration-dependent response between proteins suggest several regimes which can stabilize or aggregate gold nanoparticles without surface functionalization. Two different nanoparticle morphologies with different aggregation behaviours were combined in one "chemical nose" solution for increased discriminatory potential, as previously demonstrated only in bacteria. Using PCA, several different proteins could be distinguished at nanomolar levels based on variations in the absorbance spectra of gold nanoparticles following ambient incubation. Binary mixtures of these proteins were also distinguishable and showed trends related to the mole fraction abundance of each protein. Finally, we demonstrated a novel method of protein analysis in complex media by successfully distinguishing serum samples with and without elevated IgG levels. This technique can be further improved by including more nanoparticle morphologies, thereby increasing the variety of observable responses. Future investigations will also seek to characterize these aggregation behaviours to enhance detection capabilities for various research, clinical, and consumer-level applications.

Chapter 4

Discrimination of proteins based on interactions with surfactant-stabilized gold nanoparticles: Effects of surfactant type and concentration

4.1 Summary

Protein analysis is a fundamental aspect of biochemical research. Gold nanoparticles are an emerging platform for various biological applications given their high surface area, biocompatibility, and unique optical properties. The colorimetric properties of gold nanoparticles make them ideal for point-of-care diagnostics. Different aspects of gold nanoparticle-protein interactions have been investigated to predict the effect of protein adsorption on colloidal stability but the role of surfactants is often overlooked, despite their potential to alter both protein and nanoparticle properties. Herein, we present a method by which gold nanoparticles can be prepared in various surfactants and used for array-based quantification and identification of proteins. The exchange of surfactant not only changed the zeta potential of those gold nanoparticles, but also drastically altered their aggregation response to five different proteins (bovine serum albumin, human serum albumin, immunoglobulin G, lysozyme, and hemoglobin) in a concentration dependent manner. Finally, we demonstrate that varying surfactant concentration can be used to control assay sensitivity.

4.2 Introduction

Gold nanoparticles are a common platform for emerging nanobiosensors due to their unique optical properties and functionalizability.[3,52,113] Localized surface plasmon resonance of gold nanoparticles lends these solutions a variety of colours from orange-red to purple-blue, depending on particle size and shape.[57] Particle aggregation causes plasmon coupling and the resulting shift in colour can be visible to the unaided eye.[116] Several studies have shown how colloidal stability of gold nanoparticles can be controlled with functionalized aptamers, peptides, or antibodies to detect whole cells[132], proteins[5], nucleic acids[8], and small molecules[133,134]. While these systems offer excellent specificity due to their "lock and key" design, high synthesis complexity and probe cost limit their usefulness for broad-spectrum protein sensing.

Proteins in solution can adsorb onto nanoparticles and induce changes in colloidal stability without the need for specific probes[51,90,135]. Particle size[68,69,71,136], shape[14,40,72], surface coating[51,83,88,90], and charge[76,83] are all thought to affect how these colloidal interactions, and the resultant effects on particle

aggregation. Single-nanoparticle systems for protein quantification have been demonstrated based on this phenomenon, where the adsorption of proteins to gold nanoparticles changes their colloidal stability.[9,10,79] One group has even shown the ability to distinguish between different protein conformations.[11] The advantages of these systems over probe-based systems are lower synthesis cost and the ability to detect a wide variety of proteins. By preparing an array of different nanoparticles which respond differently to the same analyte, a "chemical nose" type sensor could generate a unique fingerprint for each analyte.[119,129] Compared to other multiplexed systems that use displacement of quenched green fluorescent protein (GFP)[117], monitoring the absorbance spectrum and aggregation of gold nanoparticles does not require the use of expensive fluorophores or a fluorescence spectrometer.

While many different aspects of gold colloid stability have been studied, the role of surfactants on protein-nanoparticle interactions is frequently overlooked. It is well known that surfactants can change nanoparticle surface properties and induce protein denaturation. Many ionic surfactants such as sodium dodecyl sulfate (SDS) and cetyltrimethylammonium bromide (CTAB) are strong denaturing agents.[137–139] Non-ionic surfactants such as Triton X and TWEEN® 20 (polysorbate 20) generally don't denature proteins.[137,140] The degree to which a protein is denatured depends on many factors including charge, hydrophobicity, and structure of the protein and surfactant.[137,141] Protein denaturation can also affect protein-nanoparticle interactions by changing the number and nature of binding sites, whether they are hydrophobic regions, charged regions, or exposed thiol groups[11]. It is therefore likely that surfactant type can influence gold nanoparticle-protein interactions and govern their colloidal stability. To our knowledge, no study has leveraged these differences for protein detection and identification. In this investigation, we demonstrate how the use of different surfactants to stabilize gold nanoparticles can affect protein-induced aggregation. We also demonstrate how several different proteins can be visually distinguished at nanomolar concentrations based on their unique response to three different surfactant-nanoparticle combinations. Finally, we show how varying the surfactant concentration can change the sensitivity across a range of protein concentrations, allowing for colorimetric assays with adjustable linear ranges. These findings have implications beyond the biosensor application, wherever the influence of biomolecules on gold nanoparticle stability may alter their behaviour.

4.3 Materials and Methods

4.3.1 Materials

Gold (III) chloride hydrate (HAuCl$_4$·xH$_2$O), CTAB, sodium borohydride, silver nitrate, hydrochloric acid, nitric acid, sodium hydroxide, L-ascorbic acid, SDS, TWEEN® 20, bovine serum albumin (BSA)(A2153), albumin from human serum (HSA)(A1653), immunoglobulin G from human

serum (IgG)(I4506), human hemoglobin (Hgb)(H7379), and lysozyme from chicken egg white (Lyz)(L6876) were purchased from Sigma-Aldrich (Oakville, ON, Canada). Trisodium citrate dihydrate and BupH phosphate buffered saline packs were purchased from Thermo Fisher Scientific (Burlington, ON, Canada). Sterile UV-star 96-well microplates, scintillation vials (20 mL), sodium chloride (ACS grade), Nalgene sterilization filter units (0.2 μm pore size), 15 mL polypropylene centrifuge tubes, and 1.7 mL polypropylene microcentrifuge tubes were purchase from VWR (Mississauga, ON, Canada). All procured chemicals were used without further purification. The 20 mL vials used for gold nanoseed synthesis were cleaned using 12M sodium hydroxide and larger glassware was cleaned using aqua regia as described in a previously published protocol.[125] Water used for the preparation of solutions was purified using a Millipore water filtration system to an electrical resistivity greater than 15 MΩ·cm. All other glass vials were triple-rinsed with Millipore water and dried completely prior to use.

4.3.2 Gold nanoparticle synthesis

Spherical CTAB-coated gold nanoparticles were synthesized according to a previously published protocol.[65] All synthesis solutions were prepared in Millipore water (>15 MΩ·cm). Briefly, gold seed precursor was prepared by adding 60 μL of ice-cold sodium borohydride to a solution containing 18.812 mL of Millipore water, 188 μL of 10 mg/mL gold (III) chloride, and 1 mL of 2 mM trisodium citrate under vigorous stirring. Following addition of sodium borohydride, the solution was stirred for 1 minute and left to mature overnight under dark ambient conditions. Nanoparticle growth solution (221.76 mL) was prepared under moderate stirring by adding 8.974 mL of 11 mM gold chloride, 1.344 mL of 5 mM silver nitrate, and 1.442 mL of 100 mM L-ascorbic acid to 210 mL of 1.47 mM CTAB. Finally, 5.6 mL of gold seed precursor was added to the nanoparticle growth solution and stirred for an additional 1.5 minutes, at which point the solution was incubated overnight under dark ambient conditions. The final nanoparticle solution was pelleted via centrifugation (16000 RCF for 15 minutes) and resuspended in 1 mM CTAB solution.

4.3.3 Surfactant exchange

TWEEN® 20 and SDS-stabilized nanoparticles were prepared from CTAB stabilized nanoparticles by repeated washing and surfactant replacement. Parts of this procedure were adapted from Tebbe et al.[30], wherein CTAB was displaced from gold nanoparticles by BSA. Here, gold nanoparticles suspended in 1 mM CTAB were added dropwise under ultrasonication to an equal volume of the new concentrated surfactant (100 mM TWEEN® 20 or 100 mM SDS). Solutions were then sonicated for an additional 2 minutes prior to centrifugation for 15 minutes at 10,000 RPM. The supernatant was discarded and the nanoparticle pellets were resuspended and sonicated in a 1 mM solution of the new

surfactant. This centrifugation and resuspension process was repeated twice, with the final resuspension being in half the supernatant volume to regain original particle concentration. Nanoparticles were then characterized and tested for stability in PBS.

Gold nanoparticle solutions with different CTAB concentrations were prepared by centrifuging particles for 15 minutes at 10,000 RPM, discarding the supernatant, and resuspending the nanoparticles in a higher or lower concentration of CTAB. Since some residual solution remained after supernatant extraction, this wash step was repeated twice to bring the CTAB concentration as close as possible to the nominal value.

4.3.4 Gold nanoparticle characterization

Characterization of gold nanoparticles was performed using ultraviolet-visible (UV-Vis) spectroscopy, zeta potential, and dynamic light scattering (DLS) measurement. Absorbance spectra were collected from 300 nm to 900 nm, at 1 nm increments, on 300 µL samples in 96-well plates using an Epoch^{TM} Microplate Spectrophotometer (Winooski, VT, USA). Zeta potential and DLS measurements were performed concurrently using a Malvern Zetasizer$^®$. Prior to DLS and zeta potential measurement, samples were diluted 1:2 in 1/4X PBS (pH 7.4) to match experimental ionic conditions.

4.3.5 Preparation of protein solutions

Fresh protein solutions were prepared prior to each experiment from lyophilized powder as per supplier's instructions. Reconstitution was performed by weighing out the lyophilized powder in a microcentrifuge tube and adding the appropriate amount of sterile solvent (PBS or NaCl saline). Gentle inversion was used to promote protein dissolution and prevent denaturation from shear stress due to vortexing. Following reconstitution, protein concentrations were verified and adjusted as necessary based on A_{280} measurements. The Beer-Lambert Law (Eq. 3.1) was used to calculate molar concentrations from absorbance values using absorption parameters from the supplier (or literature where supplier values were not available) (Table 3.1).

Serial dilutions were performed to achieve protein concentrations below the linear range of the Epoch^{TM} Microplate Spectrophotometer (0.1-2.0). Protein concentrations for samples outside this range were extrapolated from the closest dilution with a reliable absorbance value. To obtain a final concentration of 150 nM, solutions were first normalized using A_{280} to a concentration of 4.5 µM. Samples were then diluted 10X to achieve a concentration of 450 nM. Following addition of 200 µL of

46

gold nanoparticle solution to 100 μL of 450 nM protein solution, the final protein concentration was 150 nM.

4.3.6 Protein-gold incubation

Concentration-dependent response and protein identification, experiments were assessed spectrophotometrically in a transparent 96-well plate. 100 μL of each protein sample or solvent control was added to the 96-well plate. 200 μL of the gold nanoparticle solution was then added to each well containing protein or control solution. Eight replicates were used for each protein-surfactant combination during protein discrimination at 150 nM. Plates were then placed on a Stovall Belly Dancer orbital shaker (Peosta, IA, USA) for 2 minutes prior to 20 hour incubation in the dark at room temperature. Following incubation, spectral scans for each well containing gold nanoparticles were obtained from 300-900 nm, in increments of 1 nm.

4.3.7 Data analysis

Normalized response was defined as a change in peak height relative to the solvent control. First, the position (in nanometers) of the control absorbance peak was determined. Absorbance values at that wavelength were then recorded for all samples. Baseline absorbance at 800 nm was then determined for each sample, including solvent controls. Peak height was calculated by subtracting the sample's baseline absorbance (800 nm) from the sample's absorbance corresponding to the control peak position (Eq. 3.2). Peak heights were then normalized against the control to obtain a normalized response for each protein sample (Eq. 3.3).

Protein classification was done in R using the FactoMineR package for Multiple Factor Analysis (MFA).[142] Each protein assayed consisted of 3 datasets (1 spectrum for each surfactant). Each spectrum was treated as a separate category in MFA. All figures were plotted using OriginPro. Photographs were taken using a Canon EOS Rebel T3 digital camera.

4.4 Results and Discussion
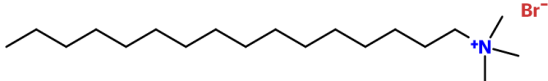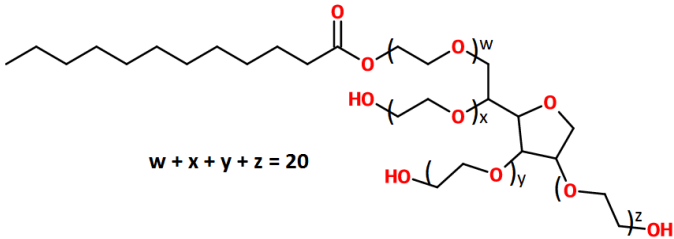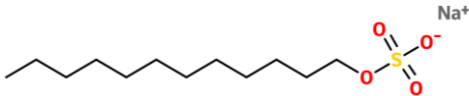
4.4.1 Surfactant exchange

We prepared three nanoparticle solutions, each with a different surfactant to study the surfactant's effect on the colloidal stability of gold nanoparticles. The cationic surfactant CTAB was used to stabilize nanoparticles during their synthesis. A 1 mM surfactant concentration was chosen based on preliminary experiments since this value was close to the minimum concentration required to maintain colloidal stability in saline. TWEEN® 20 and SDS were chosen as model nonionic and anionic

surfactants respectively. A common strategy for displacement of CTAB takes advantage of strong thiol-gold interactions.[143] However, displacement by non-thiolated molecules is possible. It has recently been confirmed through surface-enhanced Raman spectroscopy (SERS) that complete displacement of CTAB by BSA on the surface of gold nanoparticles can be achieved without nanoparticle aggregation.[30] Using a similar strategy, dropwise addition of CTAB coated nanoparticles into high concentrations of TWEEN® 20 or SDS while under ultrasonication was found to produce stable nanoparticles with negligible changes in absorption spectra. When resuspended in 1 mM solutions of their respective surfactant, these solutions were also stable under moderate ionic conditions (addition of 100 µL 1/4X PBS to 200 µL nanoparticle solution).

CTAB is a cationic surfactant due to its quaternary ammonium cation. As a result, CTAB-stabilized gold nanoparticles are cationic.[65] Due to the nonionic and anionic nature of TWEEN® 20 and SDS respectively, nanoparticles coated with these surfactants should adopt neutral and negative zeta potentials at pH 7.4. The results of zeta potential measurements at pH 7.4 are shown in Table 4.1. Reversal of zeta potential from +25.7 mV for CTAB-stabilized particles to -46.5 mV for SDS-stabilized particles matches the predicted outcome based on surfactant charge. While nanoparticles stabilized with nonionic TWEEN® 20 still possessed an electrostatic potential of approximately -16.2 mV, the polarity was inverted compared to CTAB-stabilized particles and the magnitude of this potential was smaller than that of anionic SDS. Despite predictions of a neutral particle given to the anionic nature of TWEEN® 20, these results reflect other studies where zeta potential of TWEEN® 20 coated gold nanoparticles were studied.[144–146]

Table 4.1 Surfactant structures and zeta potentials of gold nanoparticles after being stabilized with 1 mM CTAB, 1 mM TWEEN® 20, or 1 mM SDS. Zeta potentials measured following 1:2 dilution in 1/4X PBS (pH 7.4).

Surfactant	Structure	Type	NP Zeta Potential (pH 7.4)
CTAB		Cationic	25.7 mV
TWEEN® 20		Non-ionic	-16.2 mV
SDS		Anionic	-46.5 mV

The process of surfactant exchange instead of *de novo* synthesis with different surfactants was chosen to preserve the size and morphology of the gold cores, as both these parameters can impact nanoparticles-protein interactions. DLS results indicate the average particle diameters were similar (Table 4.2). Slight variations were likely due to minor aggregation during the washing and centrifugation process.

Table 4.2 DLS measurements for gold nanoparticles suspended in CTAB, Tween® 20, or SDS. Values represent the mean of three consecutive measurements (± SD).

Surfactant	Mean diameter (nm)	Polydispersity
CTAB	34.3 (±0.7)	0.20
TWEEN ®	33.1 (±0.5)	0.21
SDS	32.5 (±0.5)	0.22

This exchange of surfactant from one type to another is useful for nanoparticle characterization since it allows each nanoparticle variety to use the same gold core. While synthesis of similar nanoparticles can be achieved using different surfactants, maintaining inter-batch reproducibility while changing surfactant type would require extensive tuning and quality control or specialized purification. Using gold cores from a single process and replacing the surfactant post-synthesis helps control inter-batch variability. This technique also allows nanoparticle morphologies synthesized in a non-biocompatible surfactant to be adapted for use *in vivo*. It is interesting to note that gold nanoparticles with anionic side chains are generally considered less toxic than their cationic counterparts.[147] Furthermore, nonionic surfactants and particularly the polyoxyethylene sorbitan family (i.e. TWEEN®) have lower skin toxicity than both cationic and anionic surfactants.[148] As a result, a similar surfactant exchange strategy could be used to produce surfactant stabilized gold nanoparticles where CTAB toxicity is of concern.

4.4.2 Protein identification

Due to aggregation-dependent changes in colour, the effects of proteins on gold nanoparticle stability can be monitored visually or using a spectrophotometer. In some cases, addition of proteins has been shown to induce aggregation in a concentration-dependent response.[11,40,79] Other studies have shown that addition of proteins can actually stabilize gold nanoparticles against harsh environments (e.g. high salt conditions).[22,30] These observations are dependent upon many factors including particle size [68,69,71,136], shape [14,40,72], and charge [76,83]. When multiple proteins are assessed, the observed changes in absorption spectrum are also dependent on the protein identity.[13,14]

To assess whether proteins can be discriminated based on their interaction with surfactants, we incubated five 150 nM protein solutions (BSA, HSA, Hgb, IgG, and Lyz) with each surfactant-

nanoparticle combination and characterized their UV-Vis absorption spectra. Solutions were incubated overnight under dark ambient conditions to allow solutions ample time for colour change, however samples were noticeably different within 1 minute of incubation. The final appearance of each well is shown in Figure 4.1. In many cases, clear differences between the proteins were apparent. While the responses of BSA, Hgb, and PBS appeared similar to the unaided eye, they could be distinguished based on spectrophotometric data (Figure 4.2). Preliminary experiments in CTAB showed a concentration-dependent response to HSA and BSA from 27.46 nM to 450 µM. However, Lyz did not induce a response at any tested concentration. Unlike the response observed in CTAB, Lyz caused extensive colour shifts in TWEEN® 20 particles, whereas HSA and BSA did not. These changes in colour correspond to red-shifting and peak broadening in the absorption spectra (Figure 4.2A-C), and support the notion that the surfactant type plays a key role in modulating nanoparticle stability.
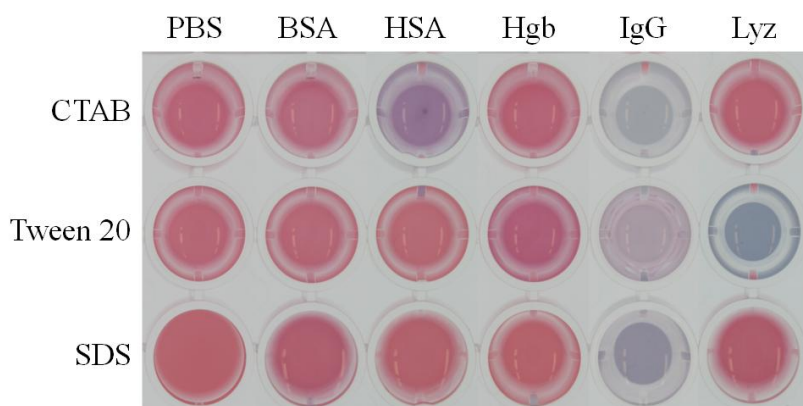
Figure 4.1 Visual appearance of gold nanoparticles with different 1 mM surfactants after 20 hour incubation with 150 nM BSA, HSA, Hgb, IgG, Lyz, or ¼X PBS (negative control).

Multiple factor analysis (MFA) was performed on the full set of UV-Vis absorption curves following the 20 hour incubation period. MFA was chosen since this extension of principal component analysis (PCA) allows each nanoparticle spectrum (CTAB, TWEEN® 20, and SDS) to be treated as distinct set of variables (i.e. separate features of the fingerprint). In this case, each surfactant-nanoparticle combination was treated as a separate dataset with 48 samples (8 replicates x 5 proteins and 1 negative control). The data from IgG dilutions were also included, from 1200 nM to 9 nM, to highlight the effect of protein concentration. The resultant biplot is shown in Figure 4.2D.
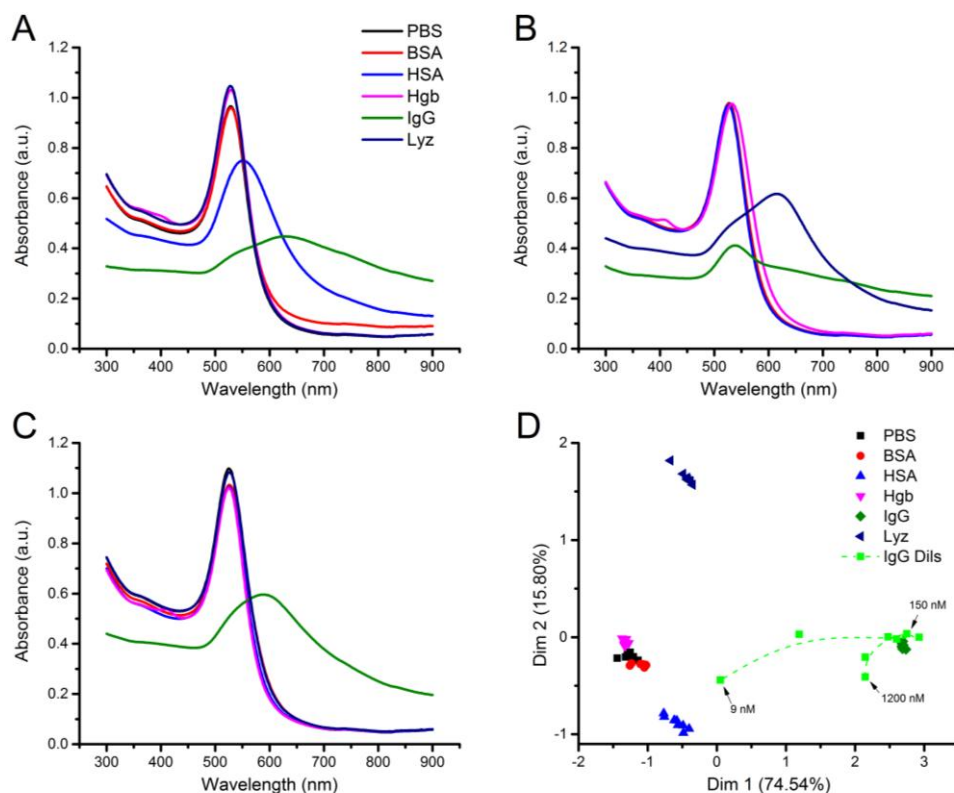
Figure 4.2 Differential response of gold nanoparticles to five different proteins at 150 nM. Average UV-Vis absorption spectra (n=8) are shown for A) CTAB-stabilized nanoparticles, B) TWEEN® 20-stabilized nanoparticles, and C) SDS-stabilized nanoparticles. D) A multiple factor analysis (MFA) plot for the combined response of all three nanoparticles to each protein at 150 nM is shown. A b-spline curve (green dash) is shown to help visualize the concentration gradient for IgG dilutions (IgG Dils) from 1200 nM to 9 nM.

The MFA biplot of five proteins and one negative control shows grouping and separation of samples based on their protein identities. The largest separation was observed for HSA, IgG, and Lyz, as these proteins produced large spectral shifts in at least one surfactant-particle combination. Weaker responses for BSA and Hgb result in grouping closer to the control. However some clustering and separation is still evident. The two principal components identified using this method could account for 90.34% of observed variability between samples.

4.4.3 Protein concentration-dependent response

IgG solutions were prepared at several concentrations to observe how protein concentration affects spectral response for the three surfactants. The resultant UV-Vis absorption curves are shown in Figure

4.3. As concentration increases from 9.4 nM to 37.5 nM, we see a decrease in absorbance for CTAB and TWEEN® 20-stabilized nanoparticles (Figure 4.3A-B). At higher concentrations (75 nM to 1200 nM) absorbance of CTAB-stabilized particles increases but the peak remains broad. Similarly, TWEEN® 20-stabilized particles increase in absorbance slightly at higher concentrations, but maintain a relatively narrow peak. In neither cases is the original absorbance peak regained at high protein concentrations. For SDS-stabilized nanoparticles (Figure 4.3C), as IgG concentration increases from 9.4 nM to 600 nM, we see an increase in absorbance, contrary to the trend for CTAB and TWEEN® 20. Absorbance then decreases slightly as IgG concentration increases from 600 nM to 1200 nM. Even at the lowest IgG concentration assayed, significant spectral shifts and broadening and were observed. The trends of increasing and decreasing absorbance as protein concentration changes reflects previous observations that nanoparticles can enter different regimes of stability depending on protein concentration[81].
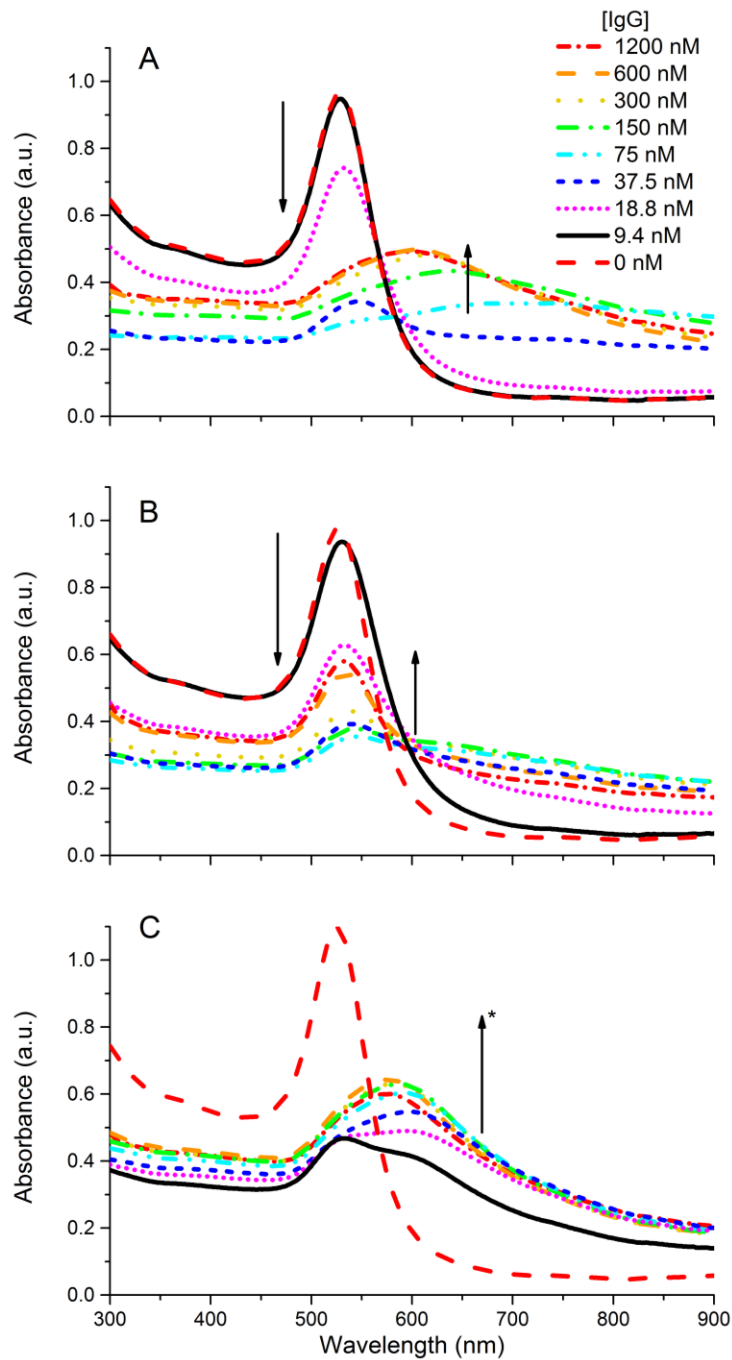
Figure 4.3 Changes in UV-Vis absorption curves of gold nanoparticles in response to different IgG concentrations. Nanoparticles were suspended in A) 1 mM CTAB, B) 1 mM Tween 20, and C) 1 mM SDS. Arrows indicate the trend in absorption following increases in protein concentration. In C), asterisk (*) indicates a decrease in absorbance as concentration increases from 600 nM to 1200 nM, contrary to the overall trend.

The spectra in Figure 4.3 were analysed using MFA and plotted alongside the 150 nM protein samples (Figure 4.2D). A b-spline curve is shown to help visualize the dilution order. The 150 nM sample agrees with previously collected replicates, indicating good reproducibility. Higher and lower dilutions of IgG indicate that the position of samples on the MFA plot relative to the PBS control is concentration-dependent. While a change in direction around 150 nM reflects the bell-shaped response, performing the assay in the linear range would allow for concurrent identification and quantification. Furthermore, noticeable spectral broadening of SDS-stabilized particles with 9.4 nM IgG suggests the potential for lower concentrations to induce changes as well, therefore the detection limit for certain proteins may be significantly lower than 9.4 nM.

4.4.4 CTAB concentration

Previous studies have shown that CTAB concentration affects the extent of BSA and HSA denaturation.[139,149] Since BSA conformation affects the extent of nanoparticle aggregation[11], it is evident that surfactant concentration should be investigated as a means of controlling the extent of nanoparticle aggregation, and may be useful for developing colorimetric assays. To assess how different concentrations of surfactant affect the protein concentration-dependent response of gold nanoparticles, we prepared CTAB-stabilized gold nanoparticles in seven different dilutions of CTAB ranging from 50 mM to 0.78 mM. Lower concentrations of CTAB were not used due to particle instability at working salt conditions. We used BSA and CTAB as models due to previous studies which characterized CTAB-dependent denaturation of BSA.[149] The normalized sample response was defined as a peak-height difference between sample and control UV-Vis absorption spectra (Eq. 3.2 and 3.3). The resultant concentration-dependent curves are shown in Figure 4.4.
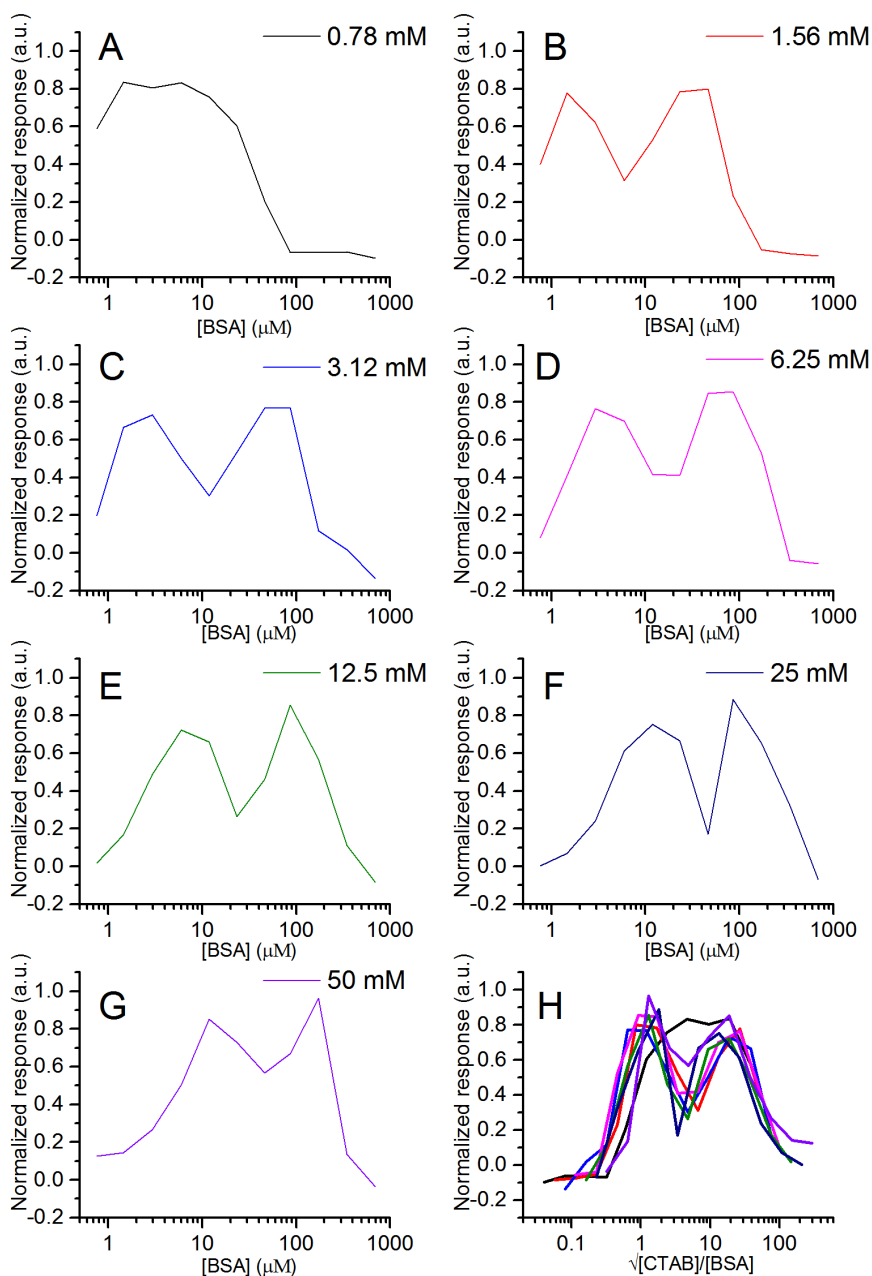
Figure 4.4 Concentration-dependent response of gold nanoparticles to BSA when suspended in varying concentrations of CTAB. Normalized response is plotted against A-G) concentration of BSA in μM and B) the ratio of $\sqrt{CTAB}$ to BSA.

One observation which few papers investigating protein-gold nanoparticle interactions report is the bell-shaped response curve. As protein concentrations increase, it has been proposed that particles pass through several regimes of stability.[81] At low concentrations, protein concentration is too low to induce nanoparticle aggregation. An increase in protein concentration induces large nanoparticle aggregates to

form. If nanoparticles are exposed instantaneously to sufficiently high protein concentrations, the surface becomes saturated with protein and a large protein corona provides steric stabilization, thereby preventing aggregation. This behaviour was only recently described with polystyrene.[81] The work by Cukalevski et al. relates this response to the number of IgG molecules per polystyrene nanoparticle. While their nanoparticles were devoid of surfactant, it is clear from Figure 4.4 that this relationship is also sensitive to surfactant concentration. A general trend emerges in Figure 4.4A, whereby increasing CTAB concentrations shift the response curve towards higher protein concentrations. In other words, higher protein concentrations are required to induce aggregation under higher CTAB concentrations. In Figure 4.4B, we see that this relationship scales approximately by $\sqrt{\text{CTAB}}$ to BSA. Ongoing studies are investigating whether this behaviour is due to competition at the gold surface between CTAB and BSA, or whether denaturation of BSA by CTAB is an important step in gold nanoparticle aggregation. However, both mechanisms may allow for tuning of sensitivity and linear range in a surfactant-based gold nanoparticle protein sensor.

Another observation with little representation in literature is the dual-peak present in concentration-dependent response curves. This may be related to different conformational states adopted by the proteins as well as their distribution and density on the nanoparticle surface, however this remains an area of ongoing investigation.

4.5 Conclusion

The effects of proteins on gold nanoparticle stability and resultant changes in absorption spectra are frequently studied for applications in biomolecular sensing. Using a simple washing procedure, we have prepared several stable gold nanoparticles in cationic, nonionic, and anionic solutions. This surfactant exchange procedure resulted in nanoparticles with varying zeta potential and maintained their stability under moderate ionic conditions. By incubating these gold nanoparticles with different proteins, we have shown how the identity and concentration of a surfactant can change the particle aggregation behaviour. We have also demonstrated how differences in response produce a unique colour and UV-Vis absorption pattern for each protein allowing for rapid visual protein identification. The effects of surfactants on nanoparticle response to proteins can therefore be exploited for multiplexed protein assays. Finally, we have shown how surfactant-coated gold nanoparticles can be a tool for studying interactions between nanoparticles and other biomolecules.

57

Chapter 5

Conclusions and Future Work

5.1 Conclusions

Over the course of this research project, we have successfully demonstrated and expanded on the use of gold nanoparticles for protein detection and identification. First, the concentration-dependent response of gold nanoparticle aggregation was characterized. Thanks to the optical properties of gold nanoparticles, this aggregation could be monitored by spectroscopy, or by visual observation. It was found that different proteins can induce aggregation of gold nanoparticles, without the need to employ specific probes such as antibodies or aptamers. Variation between proteins produced different concentration-response profiles which form the basis of protein identification and quantification. Furthermore, it was found that expanding the range of protein concentrations reveals multiple aggregation regimes, a key aspect for biosensing frequently overlooked by current literature.

Where previous studies have highlighted the effect of nanoparticle shape and size on protein-induced aggregation[14,68,69], and others have employed different gold nanoparticle shapes to detect and identify whole cells[119], we combine these concepts to develop a "chemical nose" sensor for proteins. The importance of shape was confirmed by monitoring aggregation of spherical and branched gold nanoparticles to an array of proteins. Here, each nanoparticle shape was found to produce different aggregation profiles and absorbance spectra when exposed to either BSA or IgG. By combining the response of both shapes to a single protein, we leverage those differences to improve identification. Furthermore, when two shapes are mixed in a single solution, a hybrid absorption spectrum is produced and the distinction between proteins is maintained. This allows for a simplified one-well procedure and reduces the sample volume needed to perform the assay.

This shape-based "chemical nose" was used to detect proteins in binary mixtures, as well as human serum. For binary solutions, it was shown that mixtures of HSA and IgG could be distinguished based on the ratio of HSA to IgG in solution. The observation that protein mixtures generated a response in between both pure proteins, and that similarity was dependent on the concentration of each protein suggests that relative protein concentrations could be estimated for unknown samples. Human serum represents a highly complex medium of significant clinical importance. The number of proteins in serum presents considerable challenges for quantitative and qualitative analysis due to potential interfering factors. Despite this complication, the "chemical nose" system was able to distinguish between serum samples containing a normal and clinically elevated concentration of IgG. The

development of gold-nanoparticle "chemical nose" platforms for proteins could therefore expand their use from laboratory research to clinical diagnostics.

Electrostatics play a key role in protein-nanoparticle interactions and aggregation. Additionally, it is well known that surfactants can affect protein structure and that protein structure may be related to nanoparticle aggregation[11]. To further expand on the "chemical nose" strategy, it is therefore useful to investigate new ways of increasing the difference in observed aggregation between proteins. To this end, spherical gold nanoparticles synthesized in the cationic surfactant CTAB were re-dispersed in non-ionic (Tween® 20) and anionic (SDS) surfactants. This changed their surface charge (as measured by zeta potential) while maintaining their colloidal stability in the absence of proteins.

Changing the stabilizing surfactant had a clear impact on the protein-induced aggregation profile of these particles. For instance, lysozyme did not induce any appreciable aggregation of CTAB-coated nanoparticles, while extensive aggregation of Tween® 20-coated nanoparticles was observed. When identifying proteins, good grouping and separation was achieve by assaying proteins against an array of different surfactant-stabilized gold nanoparticles. In this case, the three different nanoparticles each represent a separate input into the "chemical nose". However the array can be expanded to include any number of nanoparticle configurations. In addition to providing unique responses for protein identification, this technique of surfactant replacement is also significant since it may be used to produce stable particles with less-toxic surfactants than the currently popular CTAB. Furthermore, increasing surfactant concentration was found to shift the concentration-response profile to higher or lower concentrations. This behaviour suggests that the sensitive range of such protein assays could be adjusted simply by changing the concentration of surfactant.

5.2 Recommendations for future work

There remain many different aspects of protein-nanoparticle interactions that can be studied using the previously described methods. New discoveries can then be incorporated into protein sensing platforms to improve sensitivity, and discrimination between proteins.

Little is currently known about the role of surfactants on protein-gold nanoparticle interactions. Given the popularity of surfactants such as CTAB to synthesize shape-controlled gold nanoparticles, this topic should receive considerable attention since these results show that surfactant identity can drastically alter nanoparticle stability in the presence of proteins.

This research focused independently on the effects of shape and surfactant. However, a combination of nanoparticle shapes, sizes, and chemical coatings could further enhance the discrimination power of such assays. By generating a library of gold-nanoparticle configurations, a plethora of different responses can be obtained. Statistical efforts and machine-learning could then be applied to select the optimal combination for greatest assay performance.

The modularity of these gold-nanoparticle biosensors is one of their key features. By varying the concentration of surfactant, an added level of modularity can be added to control the linear range of these sensors. Currently, the mechanism behind this effect is not well understood. Potential explanations include the stabilizing effect of surfactants on nanoparticles, and the denaturing effect of surfactants on proteins. A better understanding of this relationship will help in the design of adjustable sensors.

Bibliography

(1)   Fasano, A.; Catassi, C. Current Approaches to Diagnosis and Treatment of Celiac Disease: An Evolving Spectrum. *Gastroenterology* **2001**, *120*, 636–651.

(2)   Manns, M. P.; Czaja, A. J.; Gorham, J. D.; Krawitt, E. L.; Mieli-Vergani, G.; Vergani, D.; Vierling, J. M. Diagnosis and Management of Autoimmune Hepatitis. *Hepatology* **2010**, *51*, 2193–2213.

(3)   Bellan, L. M.; Wu, D.; Langer, R. S. Current Trends in Nanobiosensor Technology. *Wiley Interdiscip. Rev. Nanomed. Nanobiotechnol.* **2011**, *3*, 229–246.

(4)   Jain, P. K.; El-Sayed, M. A. Plasmonic Coupling in Noble Metal Nanostructures. *Chem. Phys. Lett.* **2010**, *487*, 153–164.

(5)   Chandrawati, R.; Stevens, M. M. Controlled Assembly of Peptide-Functionalized Gold Nanoparticles for Label-Free Detection of Blood Coagulation Factor XIII Activity. *Chem. Commun.* **2014**, *50*, 5431–5434.

(6)   Daraee, H.; Pourhassanmoghadam, M.; Akbarzadeh, A.; Zarghami, N.; Rahmati-Yamchi, M. Gold Nanoparticle–oligonucleotide Conjugate to Detect the Sequence of Lung Cancer Biomarker. *Artif. Cells, Nanomedicine, Biotechnol.* **2015**, *1401*, 1–7.

(7)   Ahirwar, R.; Nahar, P. Development of a Label-Free Gold Nanoparticle-Based Colorimetric Aptasensor for Detection of Human Estrogen Receptor Alpha. *Anal. Bioanal. Chem.* **2016**, *408*, 327–332.

(8)   Gill, P.; Alvandi, A.-H.; Abdul-Tehrani, H.; Sadeghizadeh, M. Colorimetric Detection of Helicobacter Pylori DNA Using Isothermal Helicase-Dependent Amplification and Gold Nanoparticle Probes. *Diagn. Microbiol. Infect. Dis.* **2008**, *62*, 119–124.

(9)   Ho, Y. T.; Poinard, B.; Yeo, E. L. L.; Kah, J. C. Y. An Instantaneous Colorimetric Protein Assay Based on Spontaneous Formation of a Protein Corona on Gold Nanoparticles. *Analyst* **2015**, *140*, 1026–1036.

(10)   Wang, X.; Xu, Y.; Xu, X.; Hu, K.; Xiang, M.; Li, L.; Liu, F.; Li, N. Direct Determination of Urinary Lysozyme Using Surface Plasmon Resonance Light-Scattering of Gold Nanoparticles. *Talanta* **2010**, *82*, 693–697.

(11)   Deka, J.; Paul, A.; Chattopadhyay, A. Sensitive Protein Assay with Distinction of Conformations Based on Visible Absorption Changes of Citrate-Stabilized Gold Nanoparticles. *J. Phys. Chem. C* **2009**, *113*, 6936–6947.

(12) Siriwardana, K.; Wang, A.; Vangala, K.; Fitzkee, N.; Zhang, D. Probing the Effects of Cysteine Residues on Protein Adsorption onto Gold Nanoparticles Using Wild-Type and Mutated GB3 Proteins. *Langmuir* **2013**, *29*, 10990–10996.

(13) Khandelia, R.; Deka, J.; Paul, A.; Chattopadhyay, A. Signatures of Specificity of Interactions of Binary Protein Mixtures with Citrate-Stabilized Gold Nanoparticles. *RSC Adv.* **2012**, *2*, 5617–5628.

(14) Gagner, J. E.; Lopez, M. D.; Dordick, J. S.; Siegel, R. W. Effect of Gold Nanoparticle Morphology on Adsorbed Protein Structure and Function. *Biomaterials* **2011**, *32*, 7241–7252.

(15) Phillips, R. L.; Miranda, O. R.; You, C.-C.; Rotello, V. M.; Bunz, U. H. F. Rapid and Efficient Identification of Bacteria Using Gold-Nanoparticle-Poly(para-Phenyleneethynylene) Constructs. *Angew. Chem. Int. Ed. Engl.* **2008**, *47*, 2590–2594.

(16) Rana, S.; Bajaj, A.; Mout, R.; Rotello, V. M. Monolayer Coated Gold Nanoparticles for Delivery Applications. *Adv. Drug Deliv. Rev.* **2012**, *64*, 200–216.

(17) Lewinski, N.; Colvin, V.; Drezek, R. Cytotoxicity of Nanoparticles. *Small* **2008**, *4*, 26–49.

(18) Grzelczak, M.; Pérez-Juste, J.; Mulvaney, P.; Liz-Marzán, L. M. Shape Control in Gold Nanoparticle Synthesis. *Chem. Soc. Rev.* **2008**, *37*, 1783–1791.

(19) Elghanian, R.; Storhoff, J. J.; Mucic, R. C.; Letsinger, R. L.; Mirkin, C. a. Selective Colorimetric Detection of Polynucleotides Based on the Distance-Dependent Optical Properties of Gold Nanoparticles. *Science* **1997**, *277*, 1078–1081.

(20) Zhao, W.; Brook, M. a.; Li, Y. Design of Gold Nanoparticle-Based Colorimetric Biosensing Assays. *ChemBioChem* **2008**, *9*, 2363–2371.

(21) Mahmoudi, M.; Lynch, I.; Ejtehadi, M. R.; Monopoli, M. P.; Bombelli, F. B.; Laurent, S. Protein-Nanoparticle Interactions: Opportunities and Challenges. *Chem. Rev.* **2011**, *111*, 5610–5637.

(22) Dominguez-Medina, S.; Blankenburg, J.; Olson, J.; Landes, C. F.; Link, S. Adsorption of a Protein Monolayer via Hydrophobic Interactions Prevents Nanoparticle Aggregation under Harsh Environmental Conditions. *ACS Sustain Chem Eng* **2013**, *1*, 833–842.

(23) Tang, B.; Xu, S.; Tao, J.; Wu, Y.; Xu, W.; Ozaki, Y. Two-Dimensional Correlation Localized Surface Plasmon Resonance Spectroscopy for Analysis of the Interaction between Metal Nanoparticles and Bovine Serum Albumin. *J. Phys. Chem. C* **2010**, *114*, 20990–20996.

(24) Wang, A.; Vangala, K.; Vo, T.; Zhang, D.; Fitzkee, N. C. A Three-Step Model for Protein–Gold Nanoparticle Adsorption. *J. Phys. Chem. C* **2014**, *118*, 8134–8142.

(25) Casals, E.; Pfaller, T.; Duschl, A.; Oostingh, G. J.; Puntes, V. Time Evolution of the Nanoparticle Protein Corona. *ACS Nano* **2010**, *4*, 3623–3632.

(26) Lim, J. K.; Majetich, S. A.; Tilton, R. D. Stabilization of Superparamagnetic Iron Oxide Core-Gold Shell Nanoparticles in High Ionic Strength Media. *Langmuir* **2009**, *25*, 13384–13393.

(27) Ojea-Jiménez, I.; Puntes, V. Instability of Cationic Gold Nanoparticle Bioconjugates: The Role of Citrate Ions. *J. Am. Chem. Soc.* **2009**, *131*, 13320–13327.

(28) Zakaria, H. M.; Shah, A.; Konieczny, M.; Hoffmann, J. a; Nijdam, a J.; Reeves, M. E. Small Molecule- and Amino Acid-Induced Aggregation of Gold Nanoparticles. *Langmuir* **2013**, *29*, 7661–7673.

(29) Pasche, S.; Vörös, J.; Griesser, H. J.; Spencer, N. D.; Textor, M. Effects of Ionic Strength and Surface Charge on Protein Adsorption at PEGylated Surfaces Effects of Ionic Strength and Surface Charge on Protein Adsorption at PEGylated Surfaces. *J. Phys. Chem. B* **2005**, *109*, 17545–17552.

(30) Tebbe, M.; Kuttner, C.; Männel, M.; Fery, A.; Chanana, M. Colloidally Stable and Surfactant-Free Protein-Coated Gold Nanorods in Biological Media. *ACS Appl. Mater. Interfaces* **2015**, *7*, 5984–5991.

(31) Tirado-Miranda, M.; Schmitt, A.; Callejas-Fernández, J.; Fernández-Barbero, A. The Aggregation Behaviour of Protein-Coated Particles: A Light Scattering Study. *Eur. Biophys. J.* **2003**, *32*, 128–136.

(32) Du, B.; Li, Z.; Cheng, Y. Homogeneous Immunoassay Based on Aggregation of Antibody-Functionalized Gold Nanoparticles Coupled with Light Scattering Detection. *Talanta* **2008**, *75*, 959–964.

(33) Chakraborty, S.; Joshi, P.; Shanker, V.; Ansari, Z. a; Singh, S. P.; Chakrabarti, P. Contrasting Effect of Gold Nanoparticles and Nanorods with Different Surface Modifications on the Structure and Activity of Bovine Serum Albumin. *Langmuir* **2011**, *27*, 7722–7731.

(34) Khan, S.; Gupta, A.; Verma, N. C.; Nandi, C. K. Kinetics of Protein Adsorption on Gold Nanoparticle with Variable Protein Structure and Nanoparticle Size. *J. Chem. Phys.* **2015**, *143*, 164709.

(35) Pamies, R.; Cifre, J. G. H.; Espín, V. F.; Collado-González, M.; Baños, F. G. D.; De La Torre, J. G. Aggregation Behaviour of Gold Nanoparticles in Saline Aqueous Media. *J. Nanoparticle Res.* **2014**, *16*, 2376.

(36)   Salgin, S.; Salgin, U.; Bahadir, S. Zeta Potentials and Isoelectric Points of
         Biomolecules: The Effects of Ion Types and Ionic Strengths. *Int. J. Electrochem. Sci.*
         2012, *7*, 12404–12414.

(37)   Bishop, K. J. M.; Wilmer, C. E.; Soh, S.; Grzybowski, B. A. Nanoscale Forces and
         Their Uses in Self-Assembly. *Small* **2009**, *5*, 1600–1630.

(38)   Zhang, F.; Skoda, M. W. a; Jacobs, R. M. J.; Zorn, S.; Martin, R. a; Martin, C. M.;
         Clark, G. F.; Goerigk, G.; Schreiber, F. Gold Nanoparticles Decorated with
         Oligo(ethylene Glycol) Thiols: Protein Resistance and Colloidal Stability. *J. Phys.
         Chem. A* **2007**, *111*, 12229–12237.

(39)   Jamison, J. A.; Bryant, E. L.; Kadali, S. B.; Wong, M. S.; Colvin, V. L.; Matthews, K.
         S.; Calabretta, M. K. Altering Protein Surface Charge with Chemical Modification
         Modulates Protein–gold Nanoparticle Aggregation. *J. Nanoparticle Res.* **2011**, *13*, 625–
         636.

(40)   Chaudhary, A.; Gupta, A.; Khan, S.; Nandi, C. K. Morphological Effect of Gold
         Nanoparticles on the Adsorption of Bovine Serum Albumin. *Phys. Chem. Chem. Phys.*
         2014, *16*, 20471–20482.

(41)   Pan, H.; Qin, M.; Meng, W.; Cao, Y.; Wang, W. How Do Proteins Unfold upon
         Adsorption on Nanoparticle Surfaces? *Langmuir* **2012**, *28*, 12779–12787.

(42)   Yu, G.; Liu, J.; Zhou, J. Mesoscopic Coarse-Grained Simulations of Hydrophobic
         Charge Induction Chromatography (HCIC) for Protein Purification. *AIChE J.* **2015**, *61*,
         2035–2047.

(43)   Zhang, X.; Servos, M. R.; Liu, J. Ultrahigh Nanoparticle Stability against Salt, pH, and
         Solvent with Retained Surface Accessibility via Depletion Stabilization. *J. Am. Chem.
         Soc.* **2012**, *134*, 9910–9913.

(44)   Ferhan, A. R.; Guo, L.; Kim, D.-H. Influence of Ionic Strength and Surfactant
         Concentration on Electrostatic Surfacial Assembly of Cetyltrimethylammonium
         Bromide-Capped Gold Nanorods on Fully Immersed Glass. *Langmuir* **2010**, *26*, 12433–
         12442.

(45)   Abbasian, S.; Moshaii, A.; Nikkhah, M.; Farkhari, N. Adsorption of DNA on Colloidal
         Ag Nanoparticles: Effects of Nanoparticle Surface Charge, Base Content and Length of
         DNA. *Colloids Surfaces B Biointerfaces* **2014**, *116*, 439–445.

(46)   Xu, Y.; Han, T.; Li, X.; Sun, L.; Zhang, Y.; Zhang, Y. Colorimetric Detection of
         Kanamycin Based on Analyte-Protected Silver Nanoparticles and Aptamer-Selective
         Sensing Mechanism. *Anal. Chim. Acta* **2015**, *891*, 298–303.

(47)	Kjøniksen, a L.; Joabsson, F.; Thuresson, K.; Nyström, B. Salt-Induced Aggregation of Polystyrene Latex Particles in Aqueous Solutions of a Hydrophobically Modified Nonionic Cellulose Derivative and Its Unmodified Analogue. *J. Phys. Chem. B* **1999**, *103*, 9818–9825.

(48)	French, R. a.; Jacobson, A. R.; Kim, B.; Isley, S. L.; Penn, L.; Baveye, P. C. Influence of Ionic Strength, pH, and Cation Valence on Aggregation Kinetics of Titanium Dioxide Nanoparticles. *Environ. Sci. Technol.* **2009**, *43*, 1354–1359.

(49)	Bian, S. W.; Mudunkotuwa, I. a.; Rupasinghe, T.; Grassian, V. H. Aggregation and Dissolution of 4 Nm ZnO Nanoparticles in Aqueous Environments: Influence of pH, Ionic Strength, Size, and Adsorption of Humic Acid. *Langmuir* **2011**, *27*, 6059–6068.

(50)	Metin, C. O.; Lake, L. W.; Miranda, C. R.; Nguyen, Q. P. Stability of Aqueous Silica Nanoparticle Dispersions. *J. Nanoparticle Res.* **2011**, *13*, 839–850.

(51)	Boulos, S. P.; Davis, T. a; Yang, J. A.; Lohse, S. E.; Alkilany, A. M.; Holland, L. a; Murphy, C. J. Nanoparticle-Protein Interactions: A Thermodynamic and Kinetic Study of the Adsorption of Bovine Serum Albumin to Gold Nanoparticle Surfaces. *Langmuir* **2013**, *29*, 14984–14996.

(52)	Verma, M. S.; Rogowski, J. L.; Jones, L.; Gu, F. X. Colorimetric Biosensing of Pathogens Using Gold Nanoparticles. *Biotechnol. Adv.* **2015**, *33*, 666–680.

(53)	Dobrovolskaia, M. a.; Patri, A. K.; Zheng, J.; Clogston, J. D.; Ayub, N.; Aggarwal, P.; Neun, B. W.; Hall, J. B.; McNeil, S. E. Interaction of Colloidal Gold Nanoparticles with Human Blood: Effects on Particle Size and Analysis of Plasma Protein Binding Profiles. *Nanomedicine Nanotechnology, Biol. Med.* **2009**, *5*, 106–117.

(54)	Liu, Y.; Shipton, M. K.; Ryan, J.; Kaufman, E. D.; Franzen, S.; Feldheim, D. L. Synthesis, Stability, and Cellular Internalization of Gold Nanoparticles Containing Mixed Peptide-Poly(ethylene Glycol) Monolayers. *Anal. Chem.* **2007**, *79*, 2221–2229.

(55)	Radziuk, D.; Skirtach, A.; Sukhorukov, G.; Shchukin, D.; Möhwald, H. Stabilization of Silver Nanoparticles by Polyelectrolytes and Poly(ethylene Glycol). *Macromol. Rapid Commun.* **2007**, *28*, 848–855.

(56)	Zhang, F.; Dressen, D. G.; Skoda, M. W. a.; Jacobs, R. M. J.; Zorn, S.; Martin, R. a.; Martin, C. M.; Clark, G. F.; Schreiber, F. Gold Nanoparticles Decorated with Oligo(ethylene Glycol) Thiols: Kinetics of Colloid Aggregation Driven by Depletion Forces. *Eur. Biophys. J.* **2008**, *37*, 551–561.

(57)	Jain, P. K.; Lee, K. S.; El-Sayed, I. H.; El-Sayed, M. A. Calculated Absorption and Scattering Properties of Gold Nanoparticles of Different Size, Shape, and Composition: Applications in Biological Imaging and Biomedicine. *J. Phys. Chem. B* **2006**, *110*, 7238–7248.

(58)   He, Y. Q.; Liu, S. P.; Kong, L.; Liu, Z. F. A Study on the Sizes and Concentrations of Gold Nanoparticles by Spectra of Absorption, Resonance Rayleigh Scattering and Resonance Non-Linear Scattering. *Spectrochim. Acta Part A* **2005**, *61*, 2861–2866.

(59)   Liz-Marzán, L. M. Tailoring Surface Plasmons through the Morphology and Assembly of Metal Nanoparticles. *Langmuir* **2006**, *22*, 32–41.

(60)   Sau, T. K.; Murphy, C. J. Room Temperature, High-Yield Synthesis of Multiple Shapes of Gold Nanoparticles in Aqueous Solution. *J. Am. Chem. Soc.* **2004**, *126*, 8648–8649.

(61)   Sun, Y.; Xia, Y. Shape-Controlled Synthesis of Gold and Silver Nanoparticles. *Science (80-.).* **2002**, *298*, 2176–2179.

(62)   Tréguer-Delapierre, M.; Majimel, J.; Mornet, S.; Duguet, E.; Ravaine, S. Synthesis of Non-Spherical Gold Nanoparticles. *Gold Bull.* **2008**, *41*, 195–207.

(63)   Kundu, S.; Peng, L.; Liang, H. A New Route to Obtain High-Yield Multiple-Shaped Gold Nanoparticles in Aqueous Solution Using Microwave Irradiation. *Inorg. Chem.* **2008**, *47*, 6344–6352.

(64)   Lu, X.; Dong, X.; Zhang, K.; Han, X.; Fang, X.; Zhang, Y. A Gold Nanorods-Based Fluorescent Biosensor for the Detection of Hepatitis B Virus DNA Based on Fluorescence Resonance Energy Transfer. *Analyst* **2013**, *138*, 642–650.

(65)   Verma, M. S.; Chen, P. Z.; Jones, L.; Gu, F. X. Branching and Size of CTAB-Coated Gold Nanostars Control the Colorimetric Detection of Bacteria. *RSC Adv.* **2014**, *4*, 10660–10668.

(66)   Indrasekara, a S. D. S.; Meyers, S.; Shubeita, S.; Feldman, L. C.; Gustafsson, T.; Fabris, L. Gold Nanostar Substrates for SERS-Based Chemical Sensing in the Femtomolar Regime. *Nanoscale* **2014**, 8891–8899.

(67)   Lee, K.; El-sayed, M. A. Dependence of the Enhanced Optical Scattering Efficiency Relative to That of Absorption for Gold Metal Nanorods on Aspect Ratio, Size, End-Cap Shape, and Medium Refractive Index. *J. Phys. Chem. B* **2005**, *109*, 20331–20338.

(68)   Jiang, X.; Jiang, J.; Jin, Y.; Wang, E.; Dong, S. Effect of Colloidal Gold Size on the Conformational Changes of Adsorbed Cytochrome c: Probing by Circular Dichroism, UV-Visible, and Infrared Spectroscopy. *Biomacromolecules* **2005**, *6*, 46–53.

(69)   De Paoli Lacerda, S. H.; Park, J. J.; Meuse, C.; Pristinski, D.; Becker, M. L.; Karim, A.; Douglas, J. F. Interaction of Gold Nanoparticles with Common Human Blood Proteins. *ACS Nano* **2010**, *4*, 365–379.

(70) Walkey, C. D.; Olsen, J. B.; Guo, H.; Emili, A.; Chan, W. C. W. Nanoparticle Size and Surface Chemistry Determine Serum Protein Adsorption and Macrophage Uptake. *J. Am. Chem. Soc.* **2012**, *134*, 2139–2147.

(71) Deng, Z. J.; Liang, M.; Toth, I.; Monteiro, M. J.; Minchin, R. F. Molecular Interaction of Poly(acrylic Acid) Gold Nanoparticles with Human Fibrinogen. *ACS Nano* **2012**, *6*, 8962–8969.

(72) Thioune, N.; Lidgi-Guigui, N.; Cottat, M.; Gabudean, A.-M.; Focsan, M.; Benoist, H.-M.; Astilean, S.; Chapelle, M. L. Study of Gold Nanorods–protein Interaction by Localized Surface Plasmon Resonance Spectroscopy. *Gold Bull.* **2013**, *46*, 275–281.

(73) Leff, D. V; Brandt, L.; Heath, J. R. Synthesis and Characterization of Hydrophobic, Organically- Soluble Gold Nanocrystals Functionalized with Primary Amines. *Langmuir* **1996**, *12*, 4723–4730.

(74) Joshi, H.; Shirude, P. S.; Bansal, V.; Ganesh, K. N.; Sastry, M. Isothermal Titration Calorimetry Studies on the Binding of Amino Acids to Gold Nanoparticles. *J. Phys. Chem. B* **2004**, *108*, 11535–11540.

(75) Selvakannan, P. R.; Mandal, S.; Phadtare, S.; Pasricha, R.; Sastry, M. Capping of Gold Nanoparticles by the Amino Acid Lysine Renders Them Water-Dispersible. *Langmuir* **2003**, *19*, 3545–3549.

(76) Brewer, S. H.; Glomm, W. R.; Johnson, M. C.; Knag, M. K.; Franzen, S. Probing BSA Binding to Citrate-Coated Gold Nanoparticles and Surfaces. *Langmuir* **2005**, *21*, 9303–9307.

(77) Winuprasith, T.; Chantarak, S.; Suphantharika, M.; He, L.; McClements, D. J. Alterations in Nanoparticle Protein Corona by Biological Surfactants: Impact of Bile Salts on B-Lactoglobulin-Coated Gold Nanoparticles. *J. Colloid Interface Sci.* **2014**, *426*, 333–340.

(78) Gebauer, J. S.; Malissek, M.; Simon, S.; Knauer, S. K.; Maskos, M.; Stauber, R. H.; Peukert, W.; Treuel, L. Impact of the Nanoparticle-Protein Corona on Colloidal Stability and Protein Structure. *Langmuir* **2012**, *28*, 9673–9679.

(79) Stoscheck, C. M. Protein Assay Sensitive at Nanogram Levels. *Anal. Biochem.* **1987**, *160*, 301–305.

(80) Moerz, S. T.; Kraegeloh, A.; Chanana, M.; Kraus, T. Formation Mechanism for Stable Hybrid Clusters of Proteins and Nanoparticles. *ACS Nano* **2015**, *9*, 6696–6705.

(81) Cukalevski, R.; Ferreira, S. a.; Dunning, C. J.; Berggård, T.; Cedervall, T. IgG and Fibrinogen Driven Nanoparticle Aggregation. *Nano Res.* **2015**, *8*, 2733–2743.

(82)   Choi, S.; Chae, J. A Physisorbed Interface Design of Biomolecules for Selective and Sensitive Protein Detection. *J. Assoc. Lab. Autom.* **2010**, *15*, 172–178.

(83)   Deng, Z. J.; Liang, M.; Toth, I.; Monteiro, M.; Minchin, R. F. Plasma Protein Binding of Positively and Negatively Charged Polymer-Coated Gold Nanoparticles Elicits Different Biological Responses. *Nanotoxicology* **2013**, *7*, 314–322.

(84)   Marín, M. J.; Rashid, A.; Rejzek, M.; Fairhurst, S. a; Wharton, S. a; Martin, S. R.; McCauley, J. W.; Wileman, T.; Field, R. a; Russell, D. a. Glyconanoparticles for the Plasmonic Detection and Discrimination between Human and Avian Influenza Virus. *Org. Biomol. Chem.* **2013**, *11*, 7101–7107.

(85)   Prencipe, G.; Tabakman, S. M.; Welsher, K.; Liu, Z.; Goodwin, A. P.; Zhang, L.; Henry, J.; Dai, H. PEG Branched Polymer for Functionalization of Nanomaterials with Ultralong Blood Circulation. *J. Am. Chem. Soc.* **2009**, *131*, 4783–4787.

(86)   Manson, J.; Kumar, D.; Meenan, B. J.; Dixon, D. Polyethylene Glycol Functionalized Gold Nanoparticles: The Influence of Capping Density on Stability in Various Media. *Gold Bull.* **2011**, *44*, 99–105.

(87)   Schollbach, M.; Zhang, F.; Roosen-Runge, F.; Skoda, M. W. a.; Jacobs, R. M. J.; Schreiber, F. Gold Nanoparticles Decorated with Oligo(ethylene Glycol) Thiols: Surface Charges and Interactions with Proteins in Solution. *J. Colloid Interface Sci.* **2014**, *426*, 31–38.

(88)   Dominguez-Medina, S.; McDonough, S.; Swanglap, P.; Landes, C. F.; Link, S. In Situ Measurement of Bovine Serum Albumin Interaction with Gold Nanospheres. *Langmuir* **2012**, *28*, 9131–9139.

(89)   Zhang, D.; Neumann, O.; Wang, H.; Yuwono, V. M.; Barhoumi, A.; Perham, M.; Hartgerink, J. D.; Wittung-Stafshede, P.; Halas, N. J. Gold Nanoparticles Can Induce the Formation of Protein-Based Aggregates at Physiological pH. *Nano Lett.* **2009**, *9*, 666–671.

(90)   Cui, M.; Liu, R.; Deng, Z.; Ge, G.; Liu, Y.; Xie, L. Quantitative Study of Protein Coronas on Gold Nanoparticles with Different Surface Modifications. *Nano Res.* **2013**, *7*, 345–352.

(91)   Albanese, A.; Chan, W. C. W. Effect of Gold Nanoparticle Aggregation on Cell Uptake and Toxicity. *ACS Nano* **2011**, *5*, 5478–5489.

(92)   Peng, Q.; Zhang, S.; Yang, Q.; Zhang, T.; Wei, X.-Q.; Jiang, L.; Zhang, C.-L.; Chen, Q.-M.; Zhang, Z.-R.; Lin, Y.-F. Preformed Albumin Corona, a Protective Coating for Nanoparticles Based Drug Delivery System. *Biomaterials* **2013**, *34*, 8521–8530.

(93) Rusling, J. F.; Kumar, C. V; Gutkind, J. S.; Patel, V. Measurement of Biomarker Proteins for Point-of-Care Early Detection and Monitoring of Cancer. *Analyst* **2010**, *135*, 2496–2511.

(94) Anderson, N. L. The Clinical Plasma Proteome: A Survey of Clinical Assays for Proteins in Plasma and Serum. *Clin. Chem.* **2010**, *56*, 177–185.

(95) Towbin, H.; Staehelin, T.; Gordon, J. Electrophoretic Transfer of Proteins from Polyacrylamide Gels to Nitrocellulose Sheets: Procedure and Some Applications. *Proc. Natl. Acad. Sci. U. S. A.* **1979**, *76*, 4350–4354.

(96) Shi, X.; Li, D.; Xie, J.; Wang, S.; Wu, Z.; Chen, H. Spectroscopic Investigation of the Interactions between Gold Nanoparticles and Bovine Serum Albumin. *Chinese Sci. Bull.* **2012**, *57*, 1109–1115.

(97) Deka, J.; Paul, A.; Chattopadhyay, A. Estimating Conformation Content of a Protein Using Citrate-Stabilized Au Nanoparticles. *Nanoscale* **2010**, *2*, 1405–1412.

(98) Jung, S.; Nam, J.; Hwang, S.; Park, J.; Hur, J.; Im, K.; Park, N.; Kim, S. Theragnostic pH-Sensitive Gold Nanoparticles for the Selective Surface Enhanced Raman Scattering and Photothermal Cancer Therapy. *Anal. Chem.* **2013**, *85*, 7674–7681.

(99) Wustholz, K. L.; Henry, A. I.; McMahon, J. M.; Freeman, R. G.; Valley, N.; Piotti, M. E.; Natan, M. J.; Schatz, G. C.; Duyne, R. P. Van. Structure-Activity Relationships in Gold Nanoparticle Dimers and Trimers for Surface-Enhanced Raman Spectroscopy. *J. Am. Chem. Soc.* **2010**, *132*, 10903–10910.

(100) Huang, X.; Jain, P. K.; El-Sayed, I. H.; El-Sayed, M. a. Plasmonic Photothermal Therapy (PPTT) Using Gold Nanoparticles. *Lasers Med. Sci.* **2008**, *23*, 217–228.

(101) Chithrani, B. D.; Ghazani, A. A.; Chan, W. C. W. Determining the Size and Shape Dependence of Gold Nanoparticle Uptake into Mammalian Cells. *Nano Lett.* **2006**, *6*, 662–668.

(102) Moghimi, S. M.; Hunter, A. C.; Murray, J. C. Long-Circulating and Target-Specific Nanoparticles : Theory to Practice. *Pharmacol. Rev.* **2001**, *53*, 283–318.

(103) Huang, X.; Qian, W.; El-Sayed, I. H.; El-Sayed, M. A. The Potential Use of the Enhanced Nonlinear Properties of Gold Nanospheres in Photothermal Cancer Therapy. *Lasers Surg. Med.* **2007**, *39*, 747–753.

(104) Nam, J.; Won, N.; Jin, H.; Chung, H.; Kim, S. pH-Induced Aggregation of Gold Nanoparticles for Photothermal Cancer Therapy. *J. Am. Chem. Soc.* **2009**, *131*, 13639–13645.

(105) Khandelia, R.; Jaiswal, A.; Ghosh, S. S.; Chattopadhyay, A. Gold Nanoparticle-Protein Agglomerates as Versatile Nanocarriers for Drug Delivery. *Small* **2013**, *9*, 3494–3505.

(106) Bharti, B.; Meissner, J.; Findenegg, G. H. Aggregation of Silica Nanoparticles Directed by Adsorption of Lysozyme. *Langmuir* **2011**, *27*, 9823–9833.

(107) Hortin, G. L.; Carr, S. a; Anderson, N. L. Introduction: Advances in Protein Analysis for the Clinical Laboratory. *Clinical Chemistry*. 2010, pp. 149–151.

(108) López-Barea, J.; Gómez-Ariza, J. L. Environmental Proteomics and Metallomics. *Proteomics* **2006**, *6 Suppl 1*, S51–S62.

(109) Palchetti, I.; Mascini, M. Nucleic Acid Biosensors for Environmental Pollution Monitoring. *Analyst* **2008**, *133*, 846–854.

(110) Van Hengel, A. J. Food Allergen Detection Methods and the Challenge to Protect Food-Allergic Consumers. *Anal. Bioanal. Chem.* **2007**, *389*, 111–118.

(111) Rastogi, S.; Dwivedi, P. D.; Khanna, S. K.; Das, M. Detection of Aflatoxin M1 Contamination in Milk and Infant Milk Products from Indian Markets by ELISA. *Food Control* **2004**, *15*, 287–290.

(112) Kingsmore, S. F. Multiplexed Protein Measurement: Technologies and Applications of Protein and Antibody Arrays. *Nat. Rev. Drug Discov.* **2006**, *5*, 310–320.

(113) Wang, J.; Qu, X. Recent Progress in Nanosensors for Sensitive Detection of Biomolecules. *Nanoscale* **2013**, *5*, 3589–3600.

(114) Mayer, K. M.; Hafner, J. H. Localized Surface Plasmon Resonance Sensors. *Chemical Reviews*, 2011, *111*, 3828–3857.

(115) Szunerits, S.; Boukherroub, R. Sensing Using Localised Surface Plasmon Resonance Sensors. *Chem. Commun.* **2012**, *48*, 8999.

(116) Ghosh, S. K.; Pal, T. Interparticle Coupling Effect on the Surface Plasmon Resonance of Gold Nanoparticles: From Theory to Applications. *Chem. Rev.* **2007**, *107*, 4797–4862.

(117) Moyano, D. F.; Rana, S.; Bunz, U. H. F.; Rotello, V. M. Gold Nanoparticle-Polymer/biopolymer Complexes for Protein Sensing. *Faraday Discuss.* **2011**, *152*, 33–42.

(118) Saptarshi, S. R.; Duschl, A.; Lopata, A. L. Interaction of Nanoparticles with Proteins: Relation to Bio-Reactivity of the Nanoparticle. *J. Nanobiotechnology* **2013**, *11*, 26.

(119) Verma, M. S.; Chen, P. Z.; Jones, L.; Gu, F. X. Chemical Nose for the Visual Identification of Emerging Ocular Pathogens Using Gold Nanostars. *Biosens. Bioelectron.* **2014**, *61*, 386–390.

(120) Hennes, E. M.; Zeniya, M.; Czaja, A. J.; Parés, A.; Dalekos, G. N.; Krawitt, E. L.; Bittencourt, P. L.; Porta, G.; Boberg, K. M.; Hofer, H.; *et al.* Simplified Criteria for the Diagnosis of Autoimmune Hepatitis. *Hepatology* **2008**, *48*, 169–176.

(121) Du, X.-J.; Tang, L.-L.; Mao, Y.-P.; Sun, Y.; Zeng, M.-S.; Kang, T.-B.; Jia, W.-H.; Lin, A.-H.; Ma, J. The Pretreatment Albumin to Globulin Ratio Has Predictive Value for Long-Term Mortality in Nasopharyngeal Carcinoma. *PLoS One* **2014**, *9*, e94473.

(122) Shibutani, M.; Maeda, K.; Nagahara, H.; Ohtani, H.; Iseki, Y.; Ikeya, T.; Sugano, K.; Hirakawa, K. The Pretreatment Albumin to Globulin Ratio Predicts Chemotherapeutic Outcomes in Patients with Unresectable Metastatic Colorectal Cancer. *BMC Cancer* **2015**, *15*, 347.

(123) Azab, B. N.; Bhatt, V. R.; Vonfrolio, S.; Bachir, R.; Rubinshteyn, V.; Alkaied, H.; Habeshy, A.; Patel, J.; Picon, A. I.; Bloom, S. W. Value of the Pretreatment Albumin to Globulin Ratio in Predicting Long-Term Mortality in Breast Cancer Patients. *Am. J. Surg.* **2013**, *206*, 764–770.

(124) Suh, B.; Park, S.; Shin, D. W.; Yun, J. M.; Keam, B.; Yang, H.-K.; Ahn, E.; Lee, H.; Park, J. H.; Cho, B. Low Albumin-to-Globulin Ratio Associated with Cancer Incidence and Mortality in Generally Healthy Adults. *Ann. Oncol.* **2014**, *25*, 2260–2266.

(125) Liu, J.; Lu, Y. Preparation of Aptamer-Linked Gold Nanoparticle Purple Aggregates for Colorimetric Sensing of Analytes. *Nat. Protoc.* **2006**, *1*, 246–252.

(126) Stoop, J. .; Zegers, B. J. .; Sander, P. C.; Ballieux, R. E. Serum Immunoglobulin Levels in Healthy Children and Adults. *Clin Exp Immunol.* **1969**, *4*, 101–112.

(127) Pfeiffer, C.; Rehbock, C.; Hühn, D.; Carrillo-Carrion, C.; de Aberasturi, D. J.; Merk, V.; Barcikowski, S.; Parak, W. J. Interaction of Colloidal Nanoparticles with Their Local Environment: The (ionic) Nanoenvironment around Nanoparticles Is Different from Bulk and Determines the Physico-Chemical Properties of the Nanoparticles. *J. R. Soc. Interface* **2014**, *11*, 20130931.

(128) Boulet, M.; Britten, M.; Lamarche, F. Aggregation of Some Food Proteins in Aqueous Dispersions: Effects of Concentration, pH and Ionic Strength. *Food Hydrocoll.* **2000**, *14*, 135–144.

(129) Verma, M. S.; Chen, P. Z.; Jones, L.; Gu, F. X. Controlling "chemical Nose" Biosensor Characteristics by Modulating Gold Nanoparticle Shape and Concentration. *Sens. Bio-Sensing Res.* **2015**, *5*, 13–18.

(130) Sau, T. K.; Rogach, A. L. Nonspherical Noble Metal Nanoparticles: Colloid-Chemical Synthesis and Morphology Control. *Adv. Mater.* **2010**, *22*, 1781–1804.

(131) Lee, J. U.; Nguyen, A. H.; Sim, S. J. A Nanoplasmonic Biosensor for Label-Free Multiplex Detection of Cancer Biomarkers. *Biosens. Bioelectron.* **2015**, *74*, 341–346.

(132) Wang, S.; Singh, A. K.; Senapati, D.; Neely, A.; Yu, H.; Ray, P. C. Rapid Colorimetric Identification and Targeted Photothermal Lysis of Salmonella Bacteria by Using Bioconjugated Oval-Shaped Gold Nanoparticles. *Chem. - A Eur. J.* **2010**, *16*, 5600–5606.

(133) Xiao, Q.; Gao, H.; Lu, C.; Yuan, Q. Gold Nanoparticle-Based Optical Probes for Sensing Aminothiols. *Trends Anal. Chem.* **2012**, *40*, 64–76.

(134) Guo, Y.; Wang, Z.; Qu, W.; Shao, H.; Jiang, X. Colorimetric Detection of Mercury, Lead and Copper Ions Simultaneously Using Protein-Functionalized Gold Nanoparticles. *Biosens. Bioelectron.* **2011**, *26*, 4064–4069.

(135) Cedervall, T.; Lynch, I.; Lindman, S.; Berggård, T.; Thulin, E.; Nilsson, H.; Dawson, K. a; Linse, S. Understanding the Nanoparticle-Protein Corona Using Methods to Quantify Exchange Rates and Affinities of Proteins for Nanoparticles. *Proc. Natl. Acad. Sci. U. S. A.* **2007**, *104*, 2050–2055.

(136) Teichroeb, J. H.; Forrest, J. a; Jones, L. W. Size-Dependent Denaturing Kinetics of Bovine Serum Albumin Adsorbed onto Gold Nanospheres. *Eur. Phys. journal. E* **2008**, *26*, 411–415.

(137) Privé, G. G. Detergents for the Stabilization and Crystallization of Membrane Proteins. *Methods* **2007**, *41*, 388–397.

(138) Kelley, D.; McClements, D. J. Interactions of Bovine Serum Albumin with Ionic Surfactants in Aqueous Solutions. *Food Hydrocoll.* **2003**, *17*, 73–85.

(139) Vlasova, I. M.; Saletsky, a. M. Investigation of Denaturation of Human Serum Albumin under Action of Cethyltrimethylammonium Bromide by Raman Spectroscopy. *Laser Phys.* **2011**, *21*, 239–244.

(140) Seddon, A. M.; Curnow, P.; Booth, P. J. Membrane Proteins, Lipids and Detergents: Not Just a Soap Opera. *Biochimica et Biophysica Acta - Biomembranes*, 2004, *1666*, 105–117.

(141) Gudiksen, K. L.; Gitlin, I.; Moustakas, D. T.; Whitesides, G. M. Increasing the Net Charge and Decreasing the Hydrophobicity of Bovine Carbonic Anhydrase Decreases the Rate of Denaturation with Sodium Dodecyl Sulfate. *Biophys. J.* **2006**, *91*, 298–310.

(142) Lê, S., Josse, J. & Husson, F. FactoMineR: An R Package for Multivariate Analysis. *J. Stat. Softw.* **2008**, *25*, 1–18.

(143) Liao, H.; Hafner, J. H. Gold Nanorod Bioconjugates. *Chem. Mater.* **2005**, *17*, 4636–4641.

(144) Bac, L. H.; Kim, J. S.; Kim, J. C. Size, Optical and Stability Properties of Gold Nanoparticles Synthesized by Electrical Explosion of Wire in Different Aqueous Media. *Rev. Adv. Mater. Sci.* **2011**, *28*, 117–121.

(145) Wang, X.; Wei, Y.; Wang, S.; Chen, L. Red-to-Blue Colorimetric Detection of Chromium via Cr (III)-Citrate Chelating Based on Tween 20-Stabilized Gold Nanoparticles. *Colloids Surfaces A Physicochem. Eng. Asp.* **2015**, *472*, 57–62.

(146) Shih, Y. C.; Ke, C. Y.; Yu, C. J.; Lu, C. Y.; Tseng, W. L. Combined Tween 20-Stabilized Gold Nanoparticles and Reduced Graphite Oxide-Fe3O4 Nanoparticle Composites for Rapid and Efficient Removal of Mercury Species from a Complex Matrix. *ACS Appl Mater Interfaces* **2014**, *6*, 17437–17445.

(147) Goodman, C. M.; McCusker, C. D.; Yilmaz, T.; Rotello, V. M. Toxicity of Gold Nanoparticles Functionalized with Cationic and Anionic Side Chains. *Bioconjug. Chem.* **2004**, *15*, 897–900.

(148) Lémery, E.; Briançon, S.; Chevalier, Y.; Bordes, C.; Oddos, T.; Gohier, A.; Bolzinger, M.-A. Skin Toxicity of Surfactants: Structure/toxicity Relationships. *Colloids Surfaces A Physicochem. Eng. Asp.* **2015**, *469*, 166–179.

(149) Vlasova, I. M.; Zhuravleva, V. V.; Saletskii, a. M. Denaturation of Bovine Serum Albumin under the Action of Cetyltrimethylammonium Bromide, according to Data from Fluorescence Analysis. *Russ. J. Phys. Chem. A* **2013**, *87*, 1027–1034.